NASA CR-122362

STAR

16

Report MCR-72-31

X-RAY SCATTERING STUDY

Robert S. Wriston and Joseph F. Froechtenigt
Space Physics Laboratory
Martin Marietta Corporation
P. O. Box 179, Mail No. 1610
Denver, Colorado 80201

February 1972

Final Report for Contract NAS 5-20287

(NASA-CR-122362) X-RAY SCATTERING STUDY Final Report R.S. Wriston, et al (Martin Marietta Corp.) Feb. 1972 85 p CSCL 20H

N72-19767

G3/24 Unclas 21089

Prepared for
GODDARD SPACE FLIGHT CENTER
Greenbelt, Maryland 20771

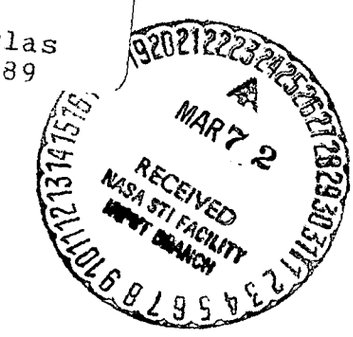

FACILITY FORM 602

(ACCESSION NUMBER)	(THRU)
85	G3
(PAGES)	(CODE)
CR-122362	24
(NASA CR OR TMX OR AD NUMBER)	(CATEGORY)

1. Report No. MCR-72-31	2. Government Accession No.	3. Recipient's Catalog No.
4. Title and Subtitle X-ray Scattering Study		5. Report Date February 1972 6. Performing Organization Code
7. Author(s) Robert S. Wriston, Joseph F. Froechtenigt		8. Performing Organization Report No.
9. Performing Organization Name and Address Space Physics Laboratory Martin Marietta Corporation P. O. Box 179, Mail No. 1610 Denver, Colorado 80201		10. Work Unit No. 11. Contract or Grant No. NAS5-20287 13. Type of Report and Period Covered Final Report
12. Sponsoring Agency Name and Address Dr. John D. Mangus Goddard Space Flight Center Greenbelt, Md. 20771		14. Sponsoring Agency Code

15. Supplementary Notes

16. Abstract

A soft X-ray glancing incidence telescope mirror and a group of twelve optical flat samples were used to study the scattering of X-rays. The mirror was made of Kanigen coated beryllium and the images produced were severely limited by scattering of X-rays. The best resolution attained was about fifteen arc seconds. The telescope efficiency was found to be 6×10^{-4}.

The X-ray beam reflected from the twelve optical flat samples was analyzed by means of a long vacuum system of special design for these tests. The scattering was found to be large in magnitude at small angles of incidence. The scattering then decreased with increasing angle of incidence until a critical angle was passed. At larger angles the scattering increased again. The samples all scattered more at 44 Å than at 8 Å. Metal samples were found to have about the same scattering at 44 Å but greater scattering at 8 A than glass samples.

17. Key Words	18. Distribution Statement		
X-ray Optics, Telescopes			
19. Security Classif. (of this report) Unclassified	20. Security Classif. (of this page) Unclassified	21. No. of Pages 85	22. Price

PREFACE

The objective of this program was to study the ability of optical surfaces to reflect and image X-rays. In any reflection of X-rays some of the beam is scattered away from the image by imperfections in the optical surfaces. If the mechanisms producing this scattering could be understood and controlled, better telescopes would result. An X-ray telescope mirror was evaluated and the properties of twelve optical flat samples were determined in the course of this program. The telescope mirror showed considerable scattering of X-rays resulting in very low telescope efficiency and poor imaging properties. The optical flat tests indicated that the scattering of X-rays was great at small angles, and decreased at larger angles of incidence until a critical angle was reached. At larger angles the scattering increased again. The phenomenon of X-ray scattering should be investigated more thoroughly with respect to angle of incidence, wavelength, polishing techniques, and theoretical modeling.

TABLE OF CONTENTS

	Page
Technical Report Standard Page	ii
Preface	iii
Table of Contents	iv
List of Figures	v
List of Tables	ix
Introduction	1
Experimental Program	4
Optical Flat Tests	4
Data Format	5
Scattering Curves	7
Nine Points Data	32
Reflecting Efficiency Measurements	42
Statistical Considerations	46
Illuminated Area of Sample	47
Samples Used in Measurements	47
Telescope Mirror Tests	49
Resolution Studies	49
Point Source Tests	53
New Technology	66
Conclusions	71
Recommendations	73
References	75

LIST OF FIGURES

	Page
Figures 1 through 24 - Scattering Curves	8
Figure 1a- Sample 1, 8 Å, 0.5°	
1b- Sample 1, 8 Å, 0.92°	
1c- Sample 1, 8 Å, 2.0°	
1d- Sample 1, 8 Å, 4.0°	
Figure 2a- Sample 2, 8 Å, 0.5°	9
2b- Sample 2, 8 Å, 0.92°	
2c- Sample 2, 8 Å, 2.0°	
2d- Sample 2, 8 Å, 4.0°	
Figure 3a- Sample 3, 8 Å, 0.5°	10
3b- Sample 3, 8 Å, 0.92°	
3c- Sample 3, 8 Å, 2.0°	
3d- Sample 3, 8 Å, 4.0°	
Figure 4a- Sample 4, 8 Å, 0.5°	11
4b- Sample 4, 8 Å, 0.92°	
4c- Sample 4, 8 Å, 2.0°	
4d- Sample 4, 8 Å, 4.0°	
Figure 5a- Sample 5, 8 Å, 0.5°	12
5b- Sample 5, 8 Å, 0.92°	
5c- Sample 5, 8 Å, 2.0°	
5d- Sample 5, 8 Å, 4.0°	
Figure 6a- Sample 6, 8 Å, 0.5°	13
6b- Sample 6, 8 Å, 0.92°	
6c- Sample 6, 8 Å, 2.0°	
6d- Sample 6, 8 Å, 4.0°	
Figure 7a- Sample 7, 8 Å, 0.5°	14
7b- Sample 7, 8 Å, 0.92°	
7c- Sample 7, 8 Å, 2.0°	
7d- Sample 7, 8 Å, 4.0°	
Figure 8a- Sample 8, 8 Å, 0.5°	15
8b- Sample 8, 8 Å, 0.92°	
8c- Sample 8, 8 Å, 2.0°	
8d- Sample 8, 8 Å, 4.0°	

Page

Figure 9a- Sample 9, 8 Å, 0.5° 16
9b- Sample 9, 8 Å, 0.92°
9c- Sample 9, 8 Å, 2.0°
9d- Sample 9, 8 Å, 4.0°

Figure 10a- Sample 7A, 8 Å, 0.5° 17
10b- Sample 7A, 8 Å, 0.92°
10c- Sample 7A, 8 Å, 2.0°
10d- Sample 7A, 8 Å, 4.0°

Figure 11a- Sample 8B, 8 Å, 0.5° 18
11b- Sample 8B, 8 Å, 0.92°
11c- Sample 8B, 8 Å, 2.0°
11d- Sample 8B, 8 Å, 4.0°

Figure 12a- Sample 9G, 8 Å, 0.5° 19
12b- Sample 9G, 8 Å, 0.92°
12c- Sample 9G, 8 Å, 2.0°
12d- Sample 9G, 8 Å, 4.0°

Figure 13a- Sample 1, 44 Å, 0.5° 20
13b- Sample 1, 44 Å, 0.92°
13c- Sample 1, 44 Å, 2.0°
13d- Sample 1, 44 Å, 4.0°

Figure 14a- Sample 2, 44 Å, 0.5° 21
14b- Sample 2, 44 Å, 0.92°
14c- Sample 2, 44 Å, 2.0°
14d- Sample 2, 44 Å, 4.0°

Figure 15a- Sample 3, 44 Å, 0.5° 22
15b- Sample 3, 44 Å, 0.92°
15c- Sample 3, 44 Å, 2.0°
15d- Sample 3, 44 Å, 4.0°

Figure 16a- Sample 4, 44 Å, 0.5° 23
16b- Sample 4, 44 Å, 0.92°
16c- Sample 4, 44 Å, 2.0°
16d- Sample 4, 44 Å, 4.0°

Figure 17a- Sample 5, 44 Å, 0.5° 24
17b- Sample 5, 44 Å, 0.92°
17c- Sample 5, 44 Å, 2.0°
17d- Sample 5, 44 Å, 4.0°

Page

Figure 18a- Sample 6, 44 Å, 0.5° 25
18b- Sample 6, 44 Å, 0.92°
18c- Sample 6, 44 Å, 2.0°
18d- Sample 6, 44 Å, 4.0°

Figure 19a- Sample 7, 44 Å, 0.5° 26
19b- Sample 7, 44 Å, 0.92°
19c- Sample 7, 44 Å, 2.0°
19d- Sample 7, 44 Å, 4.0°

Figure 20a- Sample 8, 44 Å, 0.5° 27
20b- Sample 8, 44 Å, 0.92°
20c- Sample 8, 44 Å, 2.0°
20d- Sample 8, 44 Å, 4.0°

Figure 21a- Sample 9, 44 Å, 0.5° 28
21b- Sample 9, 44 Å, 0.92°
21c- Sample 9, 44 Å, 2.0°
21d- Sample 9, 44 Å, 4.0°

Figure 22a- Sample 7A, 44 Å, 0.5° 29
22b- Sample 7A, 44 Å, 0.92°
22c- Sample 7A, 44 Å, 2.0°
22d- Sample 7A, 44 Å, 4.0°

Figure 23a- Sample 8B, 44 Å, 0.5° 30
23b- Sample 8B, 44 Å, 0.92°
23c- Sample 8B, 44 Å, 2.0°
23d- Sample 8B, 44 Å, 4.0°

Figure 24a- Sample 9G, 44 Å, 0.5° 31
24b- Sample 9G, 44 Å, 0.92°
24c- Sample 9G, 44 Å, 2.0°
24d- Sample 9G, 44 Å, 4.0°

Figure 25 - Resolution Curve 52

Figure 26 - S056-4 Telescope Point Source Test 59
Pinhole at Focal Point

Figure 27 - S056-4 Telescope Point Source Test 61
Pinhole Offset 0.020 Inches Inward

Figure 28 - S056-4 Telescope Point Source Test 62
Pinhole Offset 0.040 Inches Inward

Page

Figure 29 - SO56-4 Telescope Point Source Test Pinhole Offset 10 Arc Min from Axis 63

Figure 30 - SO56-4 Telescope Point Source Test Pinhole Offset 20 Arc Min from Axis 64

Figure 31 - X-ray Scattering Measurement Equipment 67

LIST OF TABLES

	Page
Table 1 - Nine Point Data - 8 Å - 0.5°	34
Table 2 - Nine Point Data - 8 Å - 0.92°	35
Table 3 - Nine Point Data - 8 Å - 2.0°	36
Table 4 - Nine Point Data - 8 Å - 4.0°	37
Table 5 - Nine Point Data - 44 Å - 0.5°	38
Table 6 - Nine Point Data - 44 Å - 0.92°	39
Table 7 - Nine Point Data - 44 Å - 2.0°	40
Table 8 - Nine Point Data 44 Å - 4.0°	41
Table 9 - Compilation of Scattering Width Data	43
Table 10 - Compilation of Percent Scattered Data	44
Table 11 - Compilation of Efficiency Factors	45
Table 12a - Photographic Exposure Conditions	54
b - Photographic Exposure Conditions	55
c - Photographic Exposure Conditions	56
d - Photographic Exposure Conditions	57
Table 13 - Parameters for Pinhole Tests	65

INTRODUCTION

In the visible light spectral region, astronomy can be done with telescopes of high enough quality to be called "diffraction limited". This term means that the images are limited in their quality only by the diffraction of light in the telescope optics. The same optical techniques have been applied to the making of telescopes for the soft X-ray spectral region, and this has resulted in a number of telescopes which are diffraction limited in performance when visible light tests are made. It is not, *a priori*, obvious that these telescopes will be diffraction limited when used in the soft X-ray spectral region. Indeed, it has been shown[1-4] that the limiting factor in the performance of these telescopes is the scattering of soft X-rays by the optical surfaces.

One important point learned in previous tests of soft X-ray telescopes is that the visible light tests do not predict the performance in the soft X-ray spectral region. The manufacturing techniques used were not sufficiently controlled to produce a telescope giving predictable performance. For future X-ray astronomy missions such as the HEAO, it is important to choose the optimum materials and manufacturing techniques to provide higher quality, lower cost telescopes. This program has made some of the required measurements and answered some questions regarding materials. It has also produced some questions which can only be answered by continued research into the problem.

One part of this program involved testing of a soft X-ray telescope in the same way that these telescopes were tested previously.[1-3] These tests involved inserting the telescope in a vacuum line and taking photographs of an X-ray source. These photographs were then used to evaluate the performance of the telescope mirror as a function of distance from the focal plane and the angular distance off the telescope axis. A secondary test was made in which a point source was used to study the imaging characteristics by means of a pinhole and proportional counter placed in the telescope focal plane.

The second part of this program involved measuring the properties of an X-ray beam reflected by optical flat samples as a function of wavelength and angle of incidence. Measurements of reflecting efficiency and scattering are required for a large number of sample types, and these measurements can be made at a much lower cost if optical flat samples are used. Candidate materials and optical figuring processes can be quickly evaluated in this way, and only the best surfaces used in mirror construction. Ehrenberg[5] and Elliott[6] presented an analytical model of a surface and made calculations of expected scattering. They, along with Schroeder and Klimasewski[7], presented experimental data, but this was all obtained with systems of low angular resolution and probably has little meaning in the design of grazing incidence telescopes. In order to obtain data

which are suitable for application to grazing incidence mirror construction, it is necessary to use a measurement system having angular resolution of the order of telescope resolution - one arc second or so. A total of one dozen optical flat samples were tested in the course of this work.

EXPERIMENTAL PROGRAM

During the course of this program, the scattering of X-rays by polished optical flats was measured for 12 samples, at two wavelengths (8 and 44 Å), and at four angles of incidence (0.5, 0.92, 2, and 4°). A soft X-ray telescope was also tested by taking photographs of X-ray sources and by scanning a pinhole detector across the image of a point source. The products of this program were the data recorded in the various tests. The following paragraphs in this chapter describe these data.

Optical Flat Tests

The scattering of X-rays by polished optical flats was measured by means of a special vacuum line which was approximately 36 feet long. This system will be described in more detail in the New Technology section of this report. It was necessary to use a chamber of this length in order to obtain the angular resolution required for the tests. The arrangement of the test was such that a monochromatic beam of X-rays was generated and fell on an optical flat sample at a predetermined angle of incidence. Then, the reflected beam of X-rays was scanned by a detector at a large distance (17.2 ft.). In this way the quality of the reflected beam was determined with an angular resolution of the order of one arc second.

Two types of data were collected for each case. The first was a scan of intensity values as a function of angle as the

detector was scanned across the reflected beam. Readings were taken every arc second so that the detailed shape of the scattering curve could be determined. These curves were expected to be symmetrical, but the results indicated that they were not always regular in shape. These curves were used to find the position of the peak reflected intensity, and the width of this peak was interpreted as a characteristic of the sample. The second type of data consisted of readings taken at nine selected points (0, $\pm$5, $\pm$10, $\pm$20, $\pm$30 arc seconds) about the peak. These points were used in making calculations of the percentage of radiation scattered away from the main reflected beam.

Data Format

As defined in Figure 31 of this report, the entrance and exit slit widths were initially set at .002 inch and the sample slit width was .001 inch. This configuration was found to be better than required with respect to resolution at small angles of incidence, but produced a low intensity value in the detector. A wider slit configuration was then used in order to achieve better counting statistics in a reasonable counting time (100 sec). This was .002-inch-width at the entrance slit (source), .002-inch-width at the sample, and .004-inch-width at the exit slit (detector). The narrower slit spacings were all used in the early measurements at small angles of incidence.

Those data curves made using the small slit spacings (2, 1, 2) were:

1-8-0.92, 2-8-0.5, 2-8-0.92, 3-8-0.5,

3-8-0.92, 4-8-0.5, 5-8-0.5, 5-8-0.92,

6-8-0.5, 6-8-0.92, 1-44-0.5, and 2-44-0.5.

All other measurements were made using the wider (2, 2, 4) spacings.

From geometrical considerations, assuming no scattering, the X-ray beam reflected from the sample should have a trapezoidal intensity profile that has a four arc second FWHM in the (2, 1, 2) case and an eight arc second FWHM in the (2, 2, 4) case. The detector slit width broadens the effective beam width by 2 and 4 arc seconds in the respective cases and changes their shape so that the calculated curves should be triangular with a four arc second FWHM in the (2, 1, 2) case and trapezoidal with an eight arc second FWHM in the (2, 2, 4) case. The 17.2 ft working distance was chosen so that one arc second was equal to .001 inch of linear motion. The value S was defined as the difference between the observed curve width (FWHM) and the calculated width (FWHM) based on geometrical considerations. Negative values of S are thought to be due to error in setting the slits or in the motion of the system during the course of a run. The error range in S is about ± 2 arc seconds. Calculated curves have been drawn in on Figures 19b and 24b.

As shown in the graphs in Figures 1 - 24, the negative angles are in the direction away from the surface of the sample. No systematic asymmetry was observed in the data because of the change in angle of incidence. The failure of the nine points data to be exactly symmetrical should be interpreted as an uncertainty in the position of the detector. This positional uncertainty in locating the peak was ± 3 arc seconds, but the relative locations of the nine points were uncertain by less than ± 1 arc second.

Scattering Curves

Figures 1 through 24 show the relative intensity curves obtained from the 61 point raw data. Each figure contains four graphs - one each for each angle of incidence at one wavelength for a single sample. Figures 1 through 12 are for the 8 Å radiation and Figures 13 through 24 are for the 44 Å radiation. Each individual graph contains an identification number in the upper right hand corner. The first number is the sample number, the second is the wavelength of the radiation, and the last number is the angle of incidence at which the sample was positioned. Each graph also contains a value representative of the scattering width in arc seconds, designated as S. This value was defined as the difference between the observed curve width (FWHM) and the calculated width (FWHM).

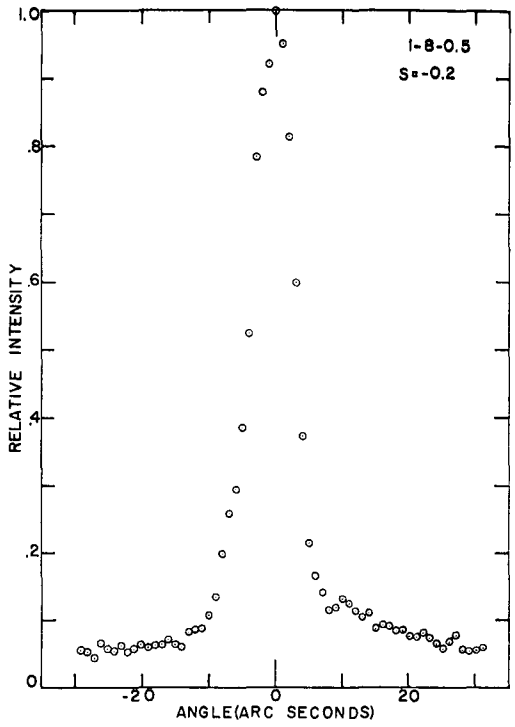

(a) 0.5 Degrees

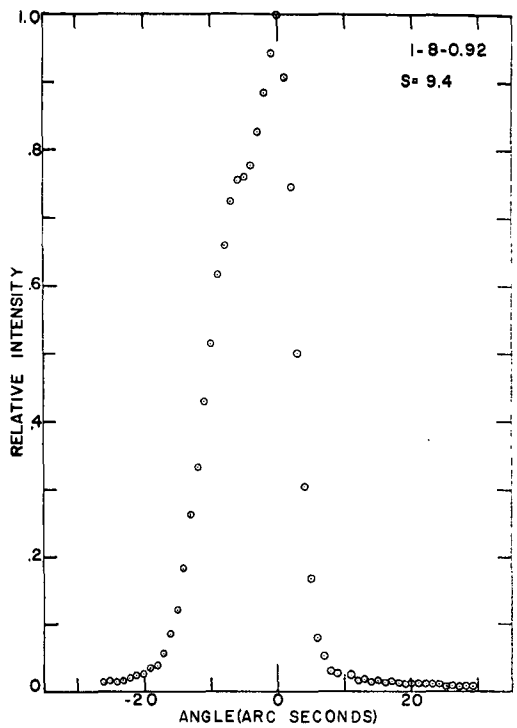

(b) 0.92 Degrees

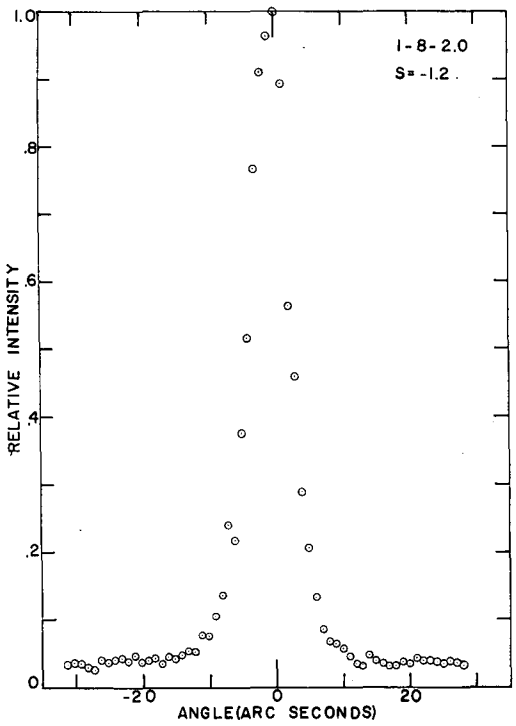

(c) 2.0 Degrees

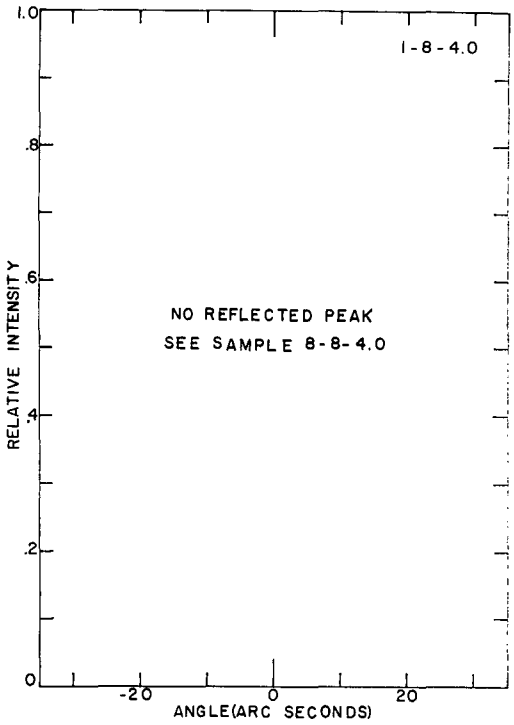

(d) 4.0 Degrees

Figure 1. Sample 1, 8 Å

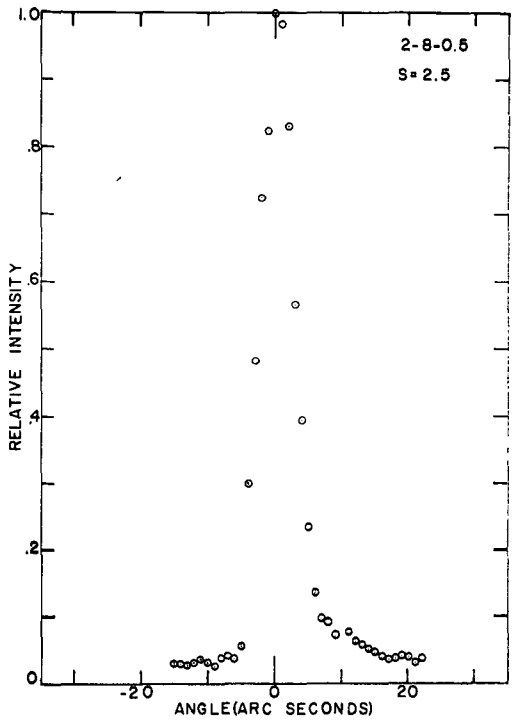

(a) 0.5 Degrees

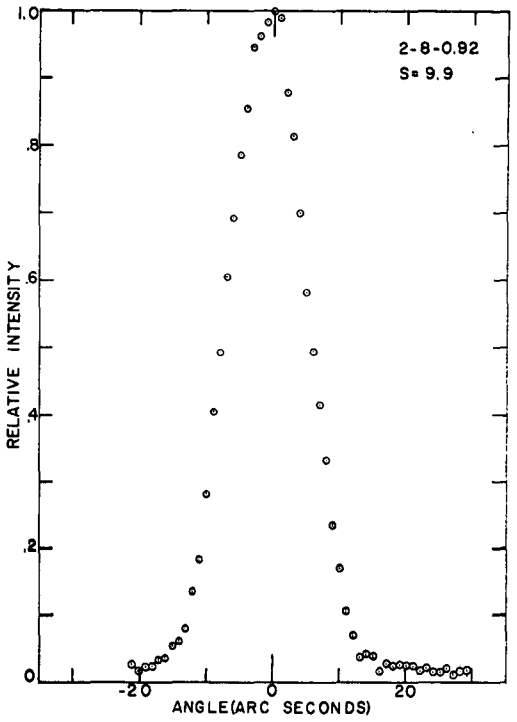

(b) 0.92 Degrees

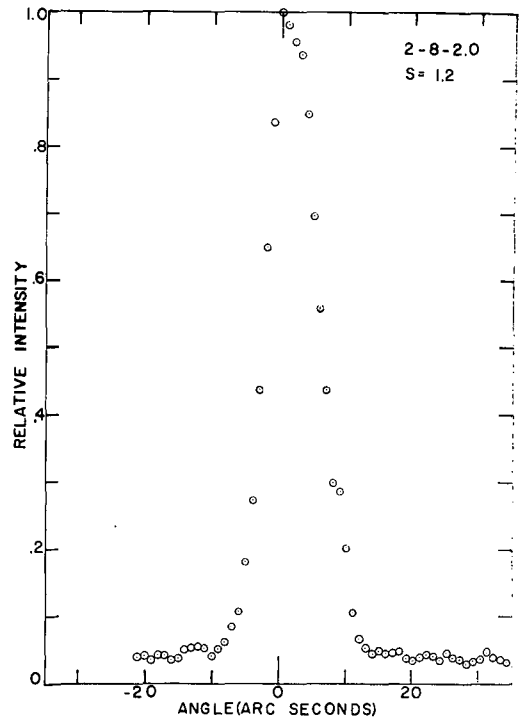

(c) 2.0 Degrees

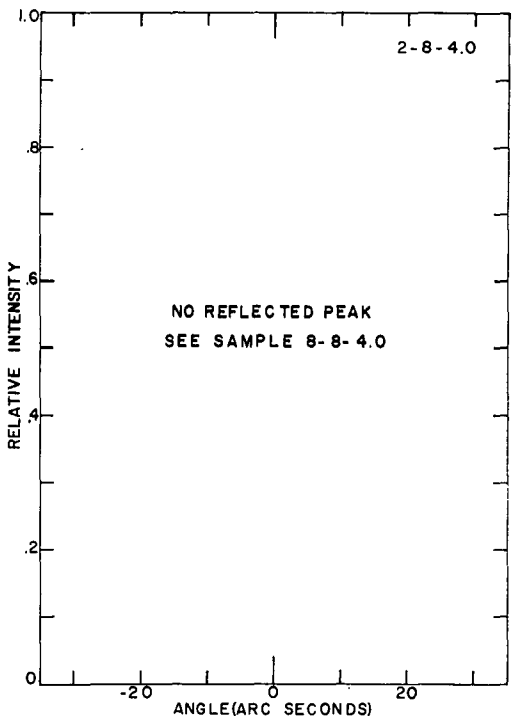

(d) 4.0 Degrees

Figure 2. Sample 2, 8 Å

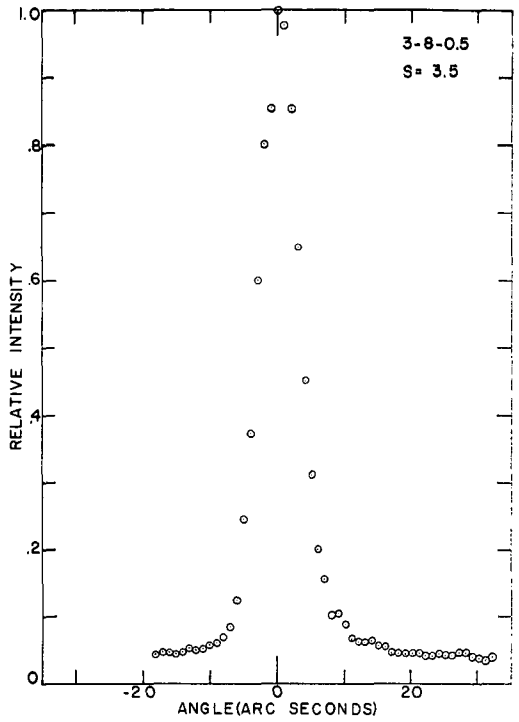

(a) 0.5 Degrees

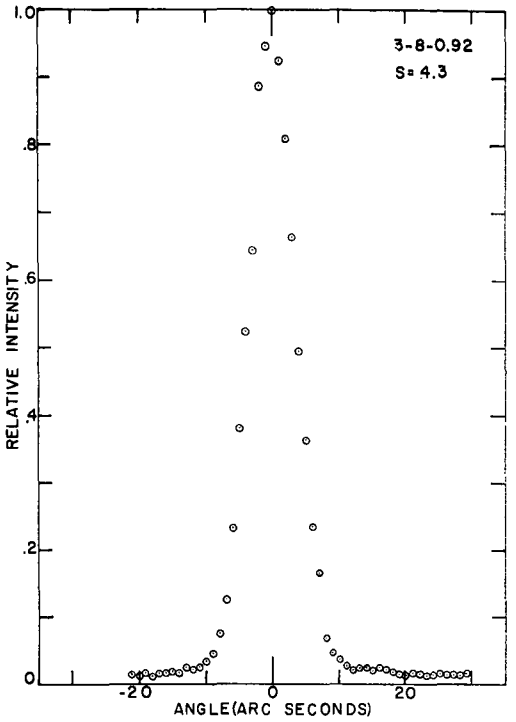

(b) 0.92 Degrees

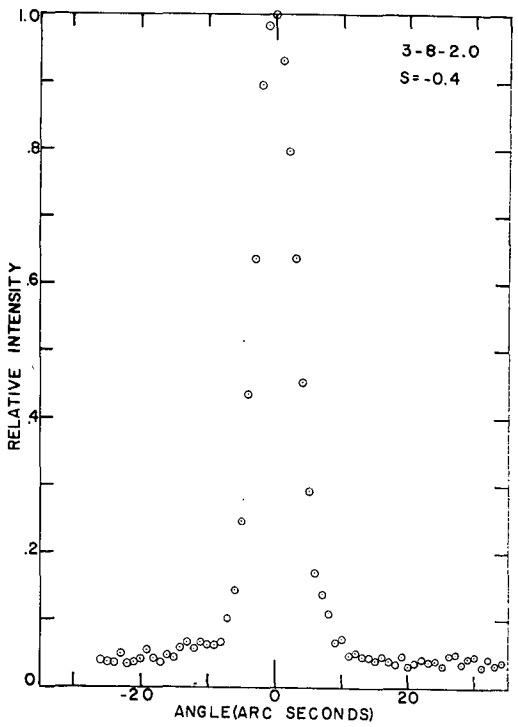

(c) 2.0 Degrees

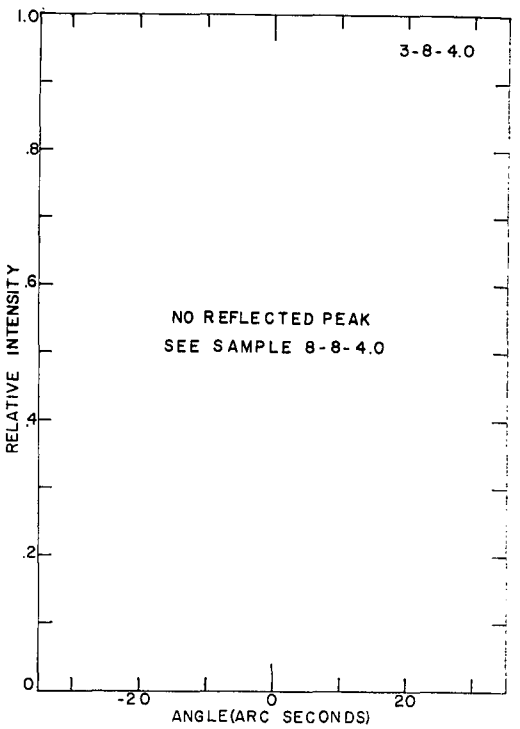

(d) 4.0 Degrees

Figure 3. Sample 3, 8 Å

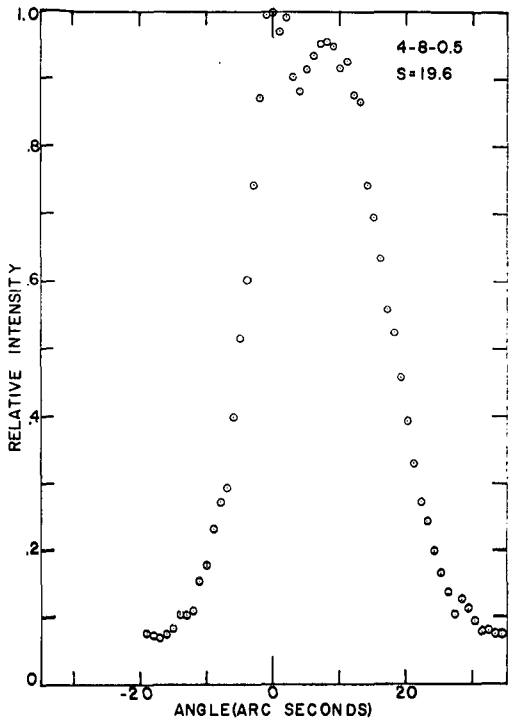

(a) 0.5 Degrees

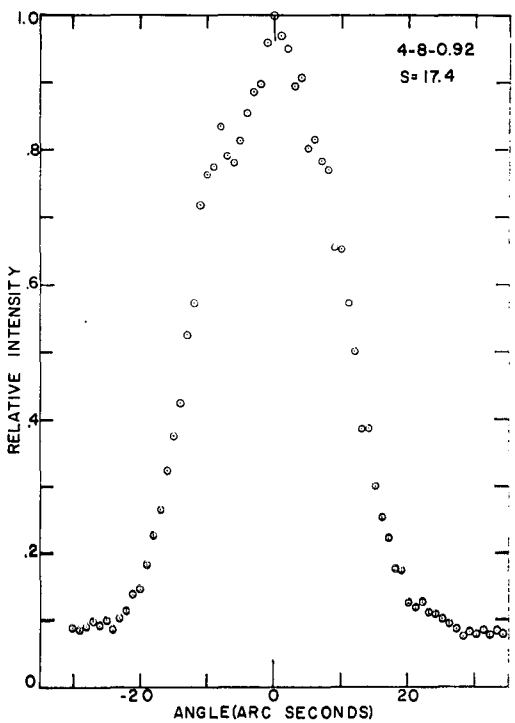

(b) 0.92 Degrees

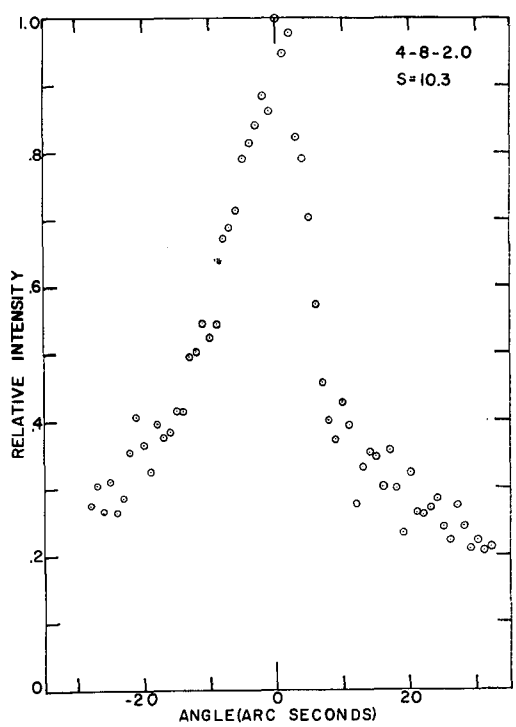

(c) 2.0 Degrees

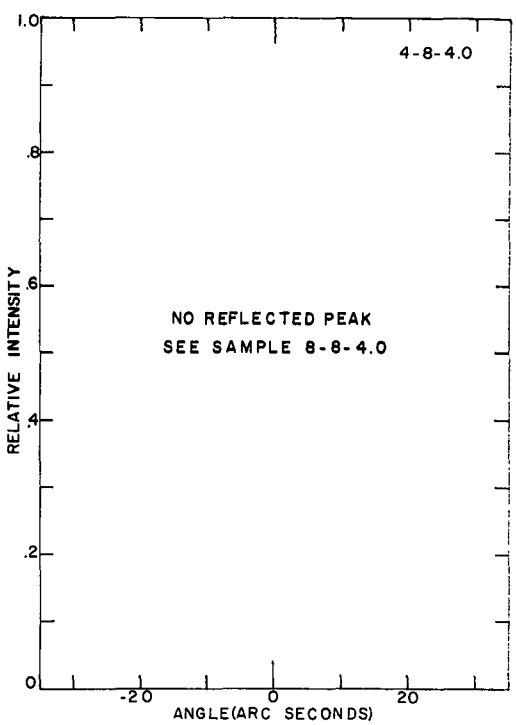

(d) 4.0 Degrees

Figure 4. Sample 4, 8 Å

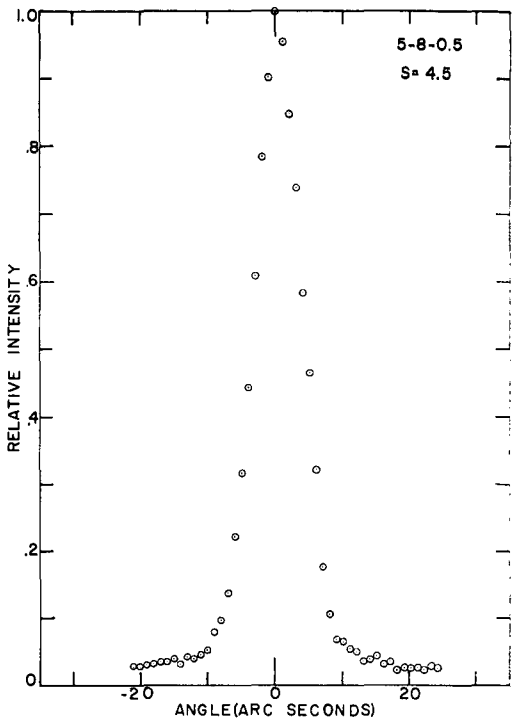

(a) 0.5 Degrees

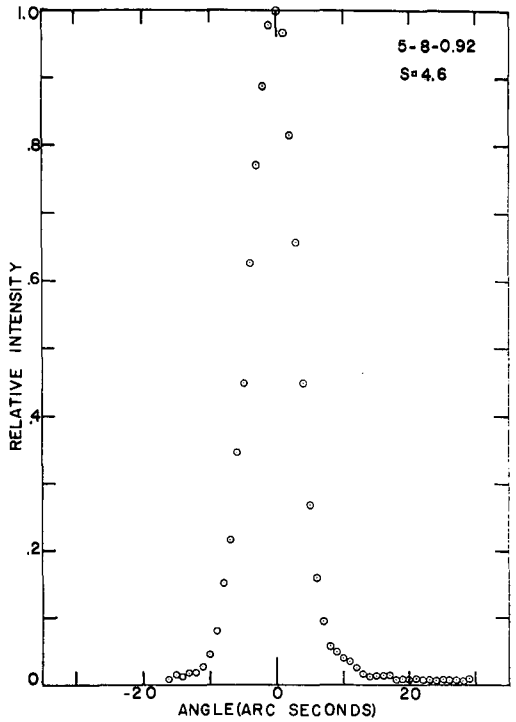

(b) 0.92 Degrees

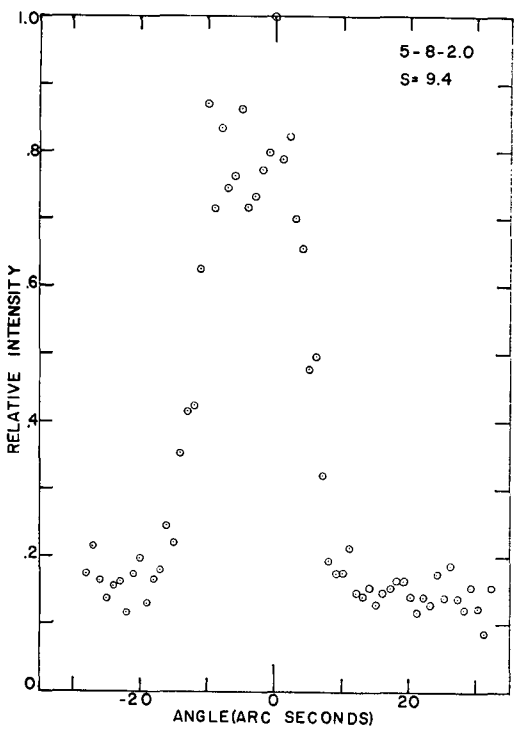

(c) 2.0 Degrees

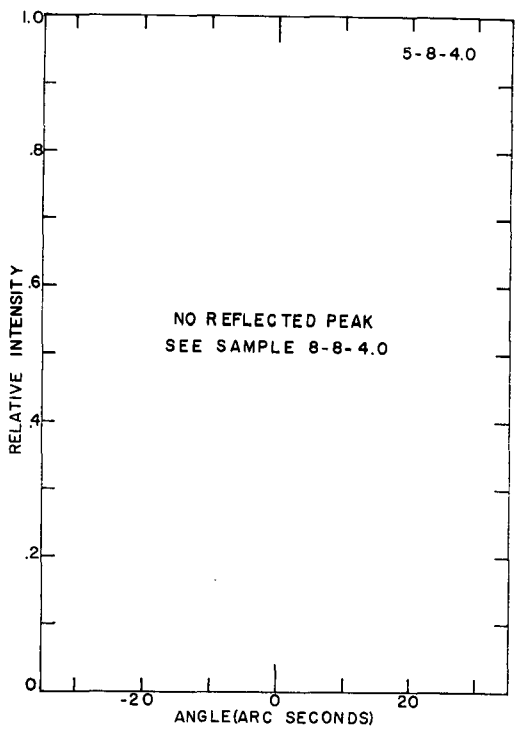

(d) 4.0 Degrees

Figure 5. Sample 5, 8 A

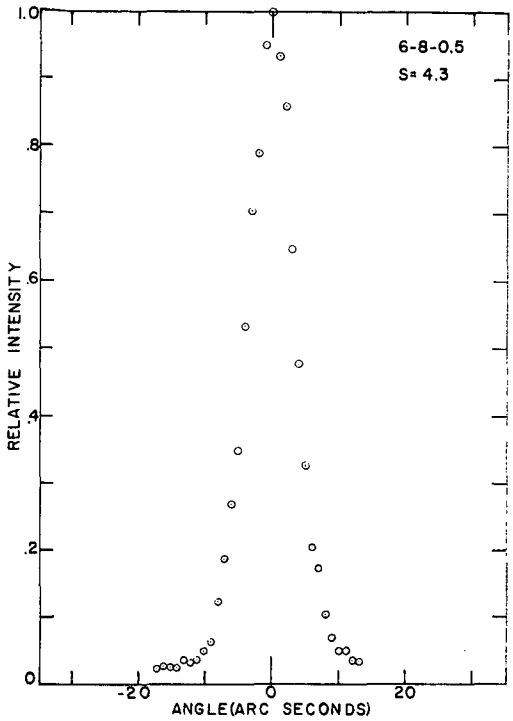

(a) 0.5 Degrees

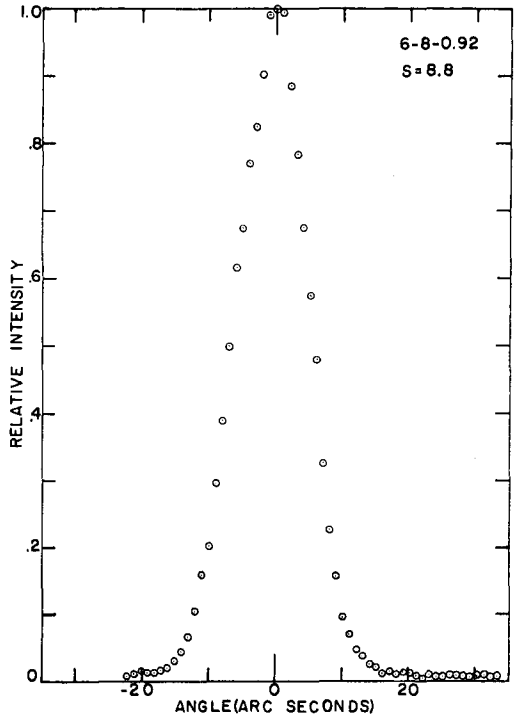

(b) 0.92 Degrees

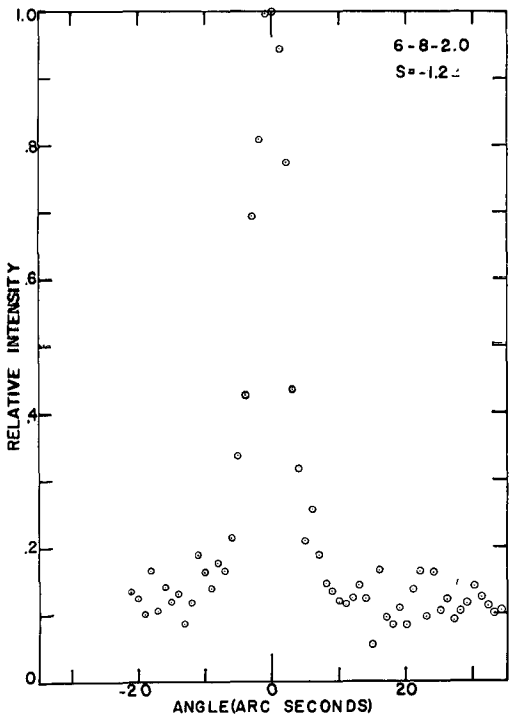

(c) 2.0 Degrees

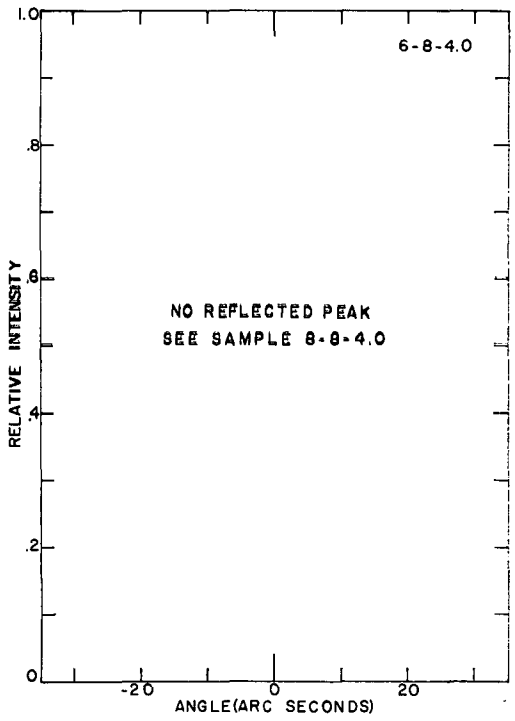

(d) 4.0 Degrees

Figure 6. Sample 6, 8 Å

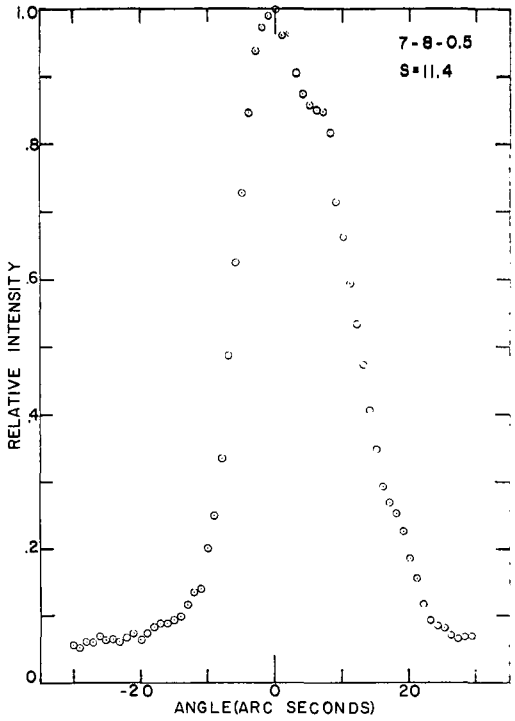

(a) 0.5 Degrees

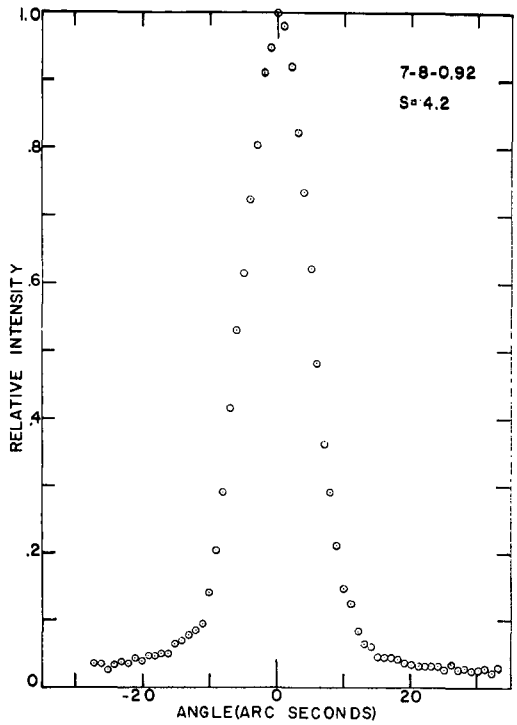

(b) 0.92 Degrees

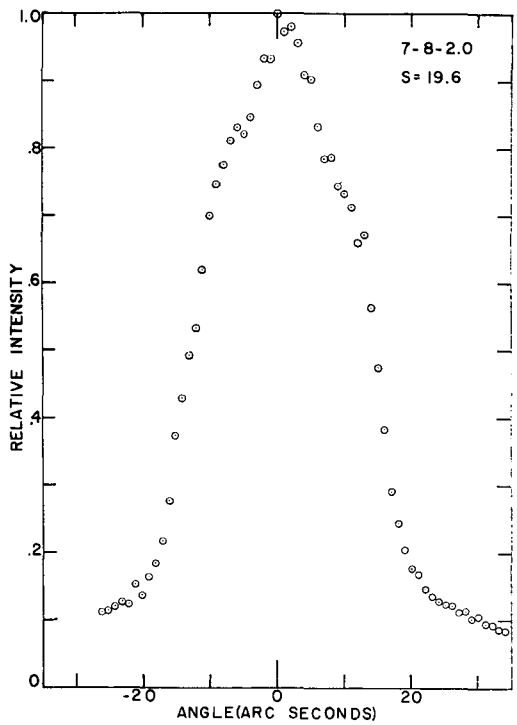

(c) 2.0 Degrees

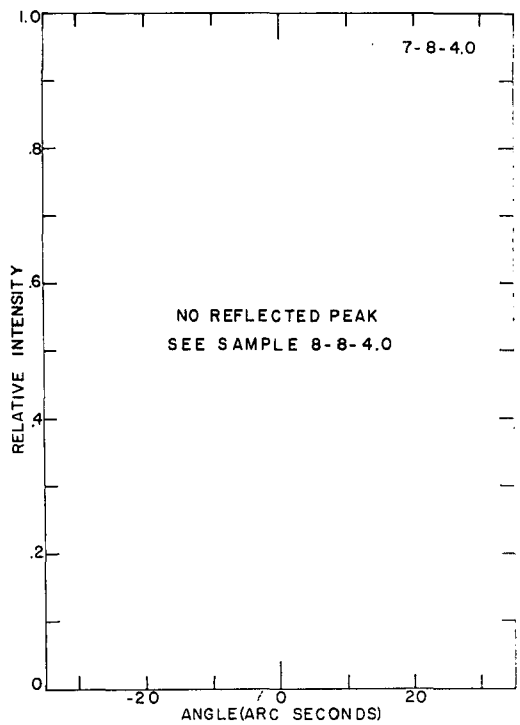

(d) 4.0 Degrees

Figure 7. Sample 7, 8 A

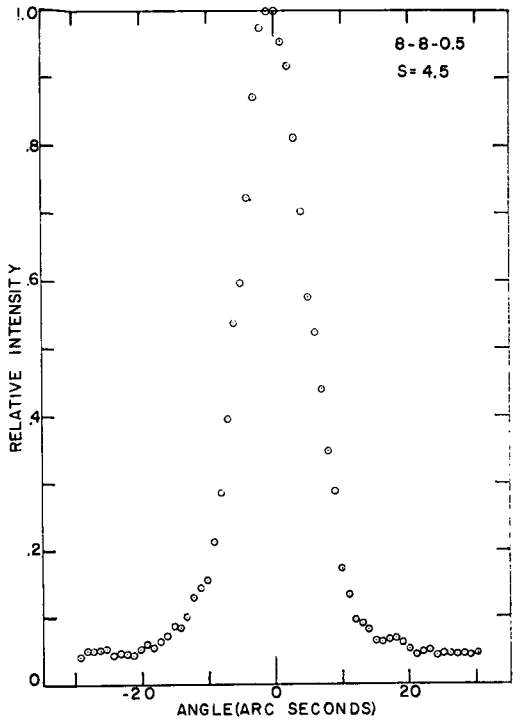

(a) 0.5 Degrees

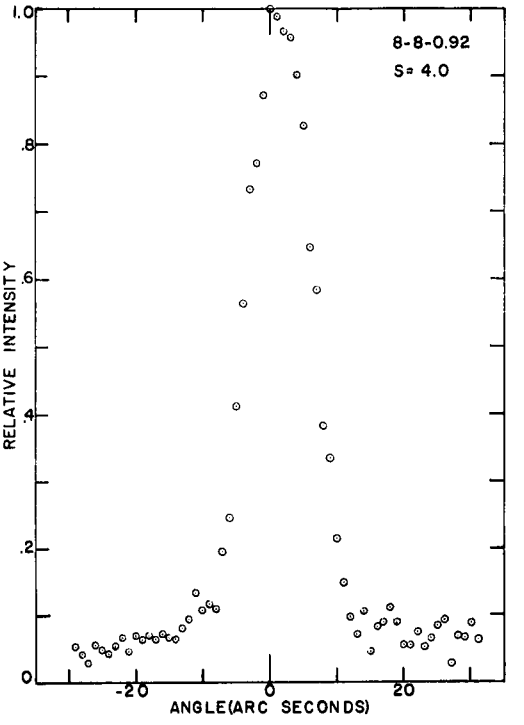

(b) 0.92 Degrees

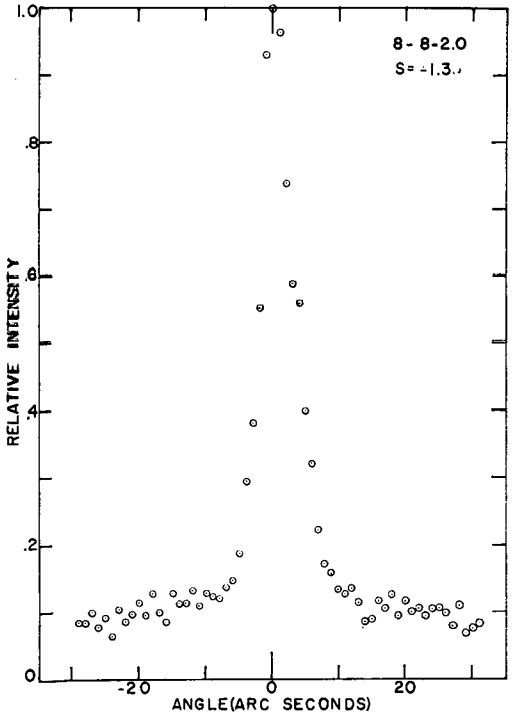

(c) 2.0 Degrees

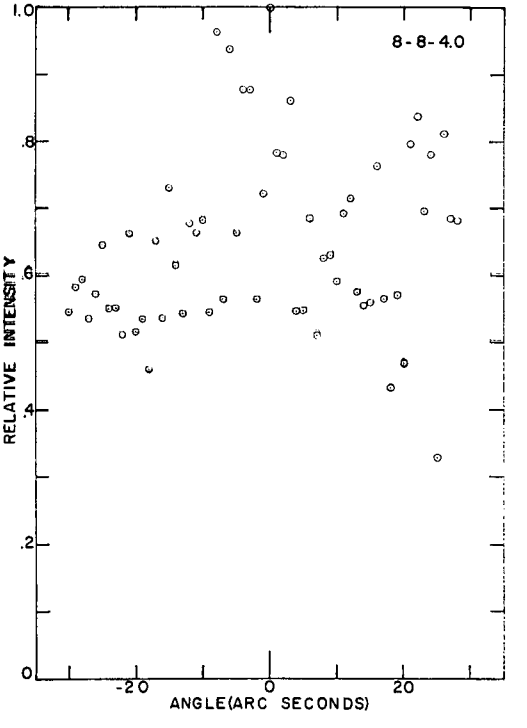

(d) 4.0 Degrees

Figure 8. Sample 8, 8 A

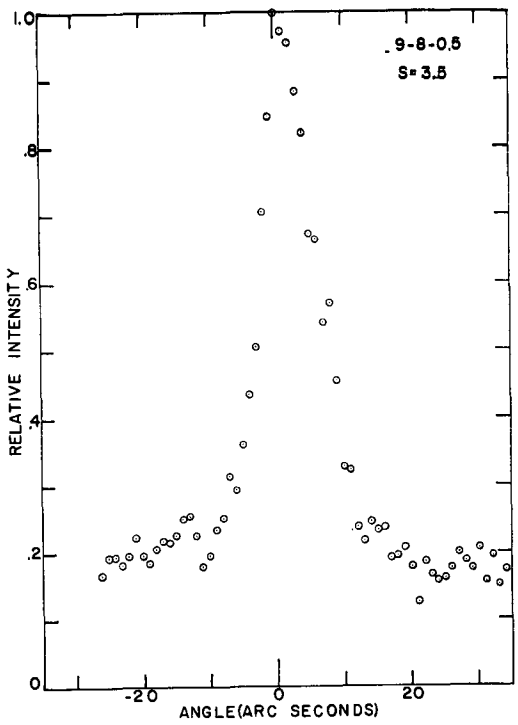

(a) 0.5 Degrees

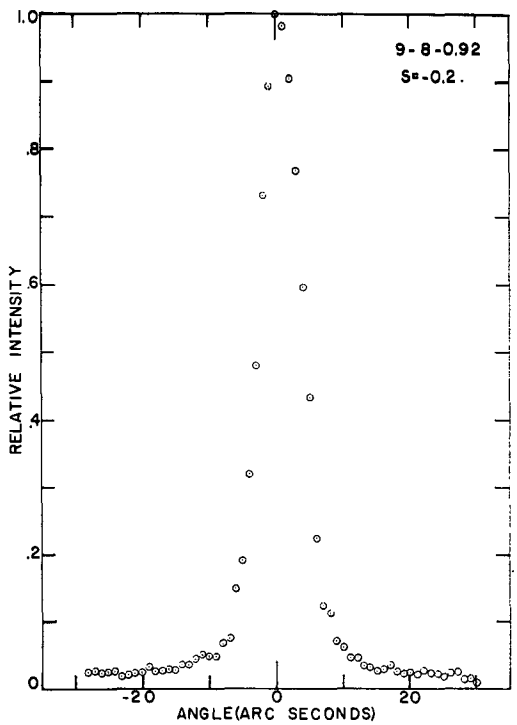

(b) 0.92 Degrees

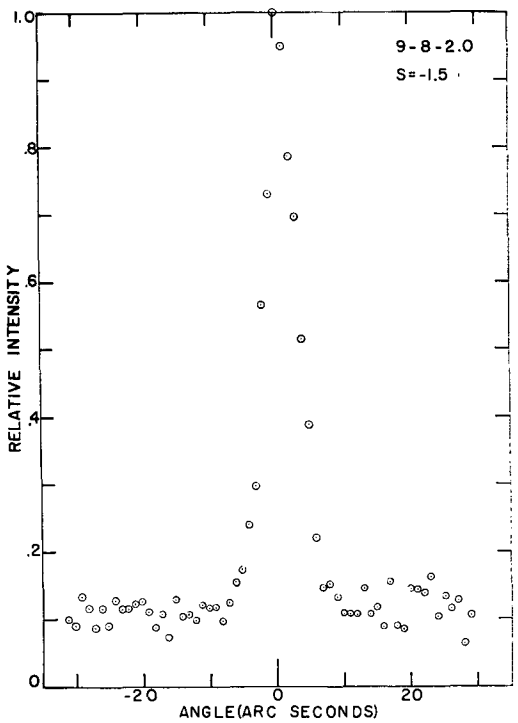

(c) 2.0 Degrees

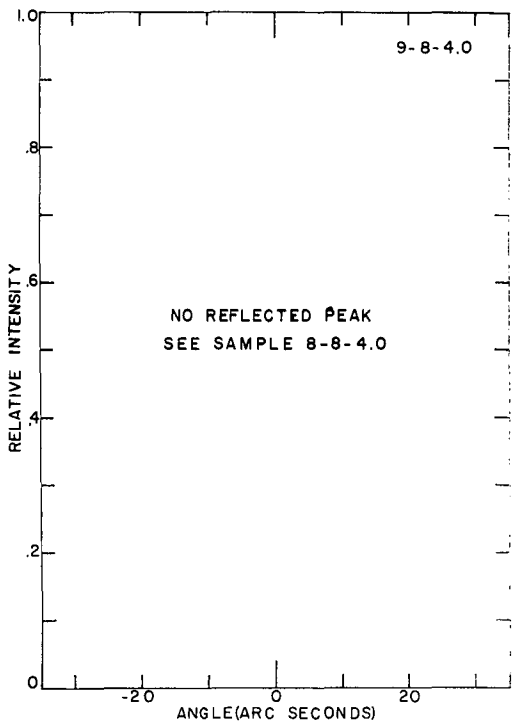

(d) 4.0 Degrees

Figure 9. Sample 9, 8 A

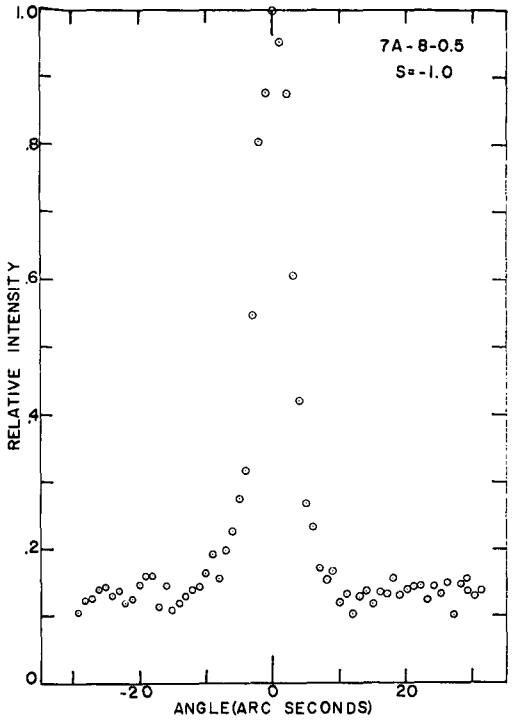

(a) 0.5 Degrees

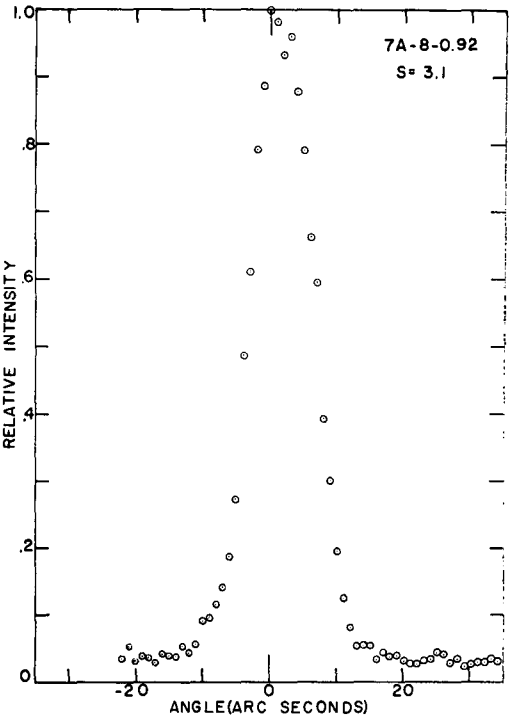

(b) 0.92 Degrees

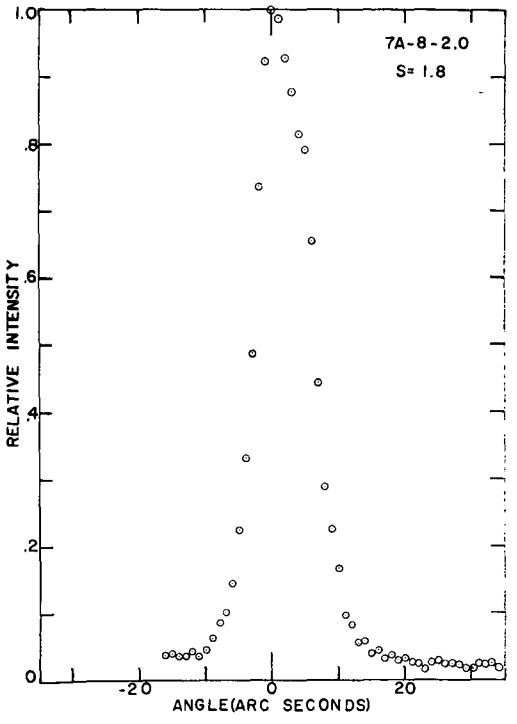

(c) 2.0 Degrees

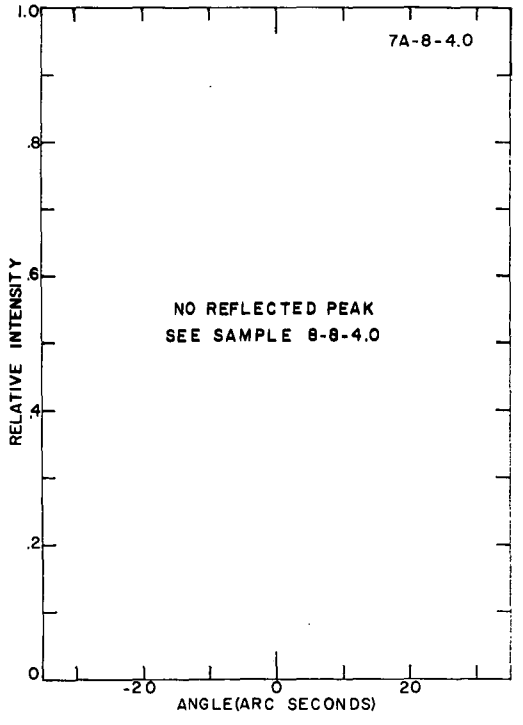

(d) 4.0 Degrees

Figure 10. Sample 7A, 8 Å

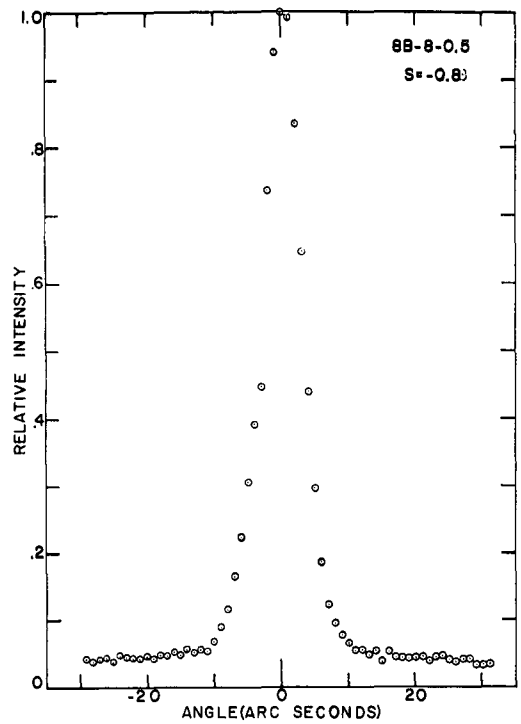

(a) 0.5 Degrees

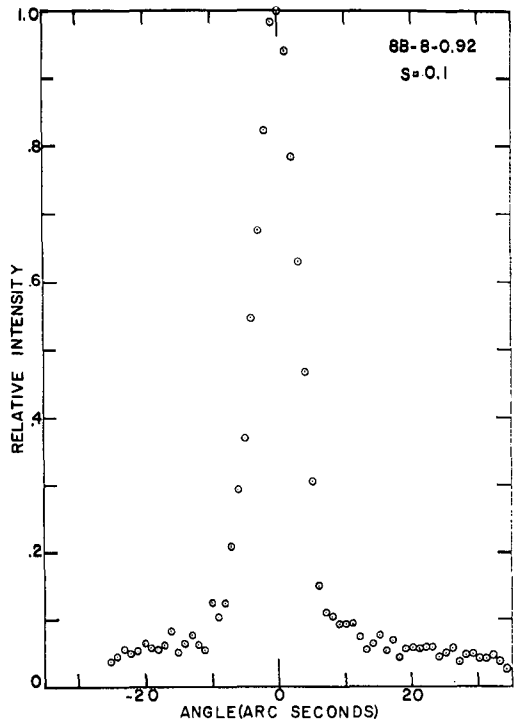

(b) 0.92 Degrees

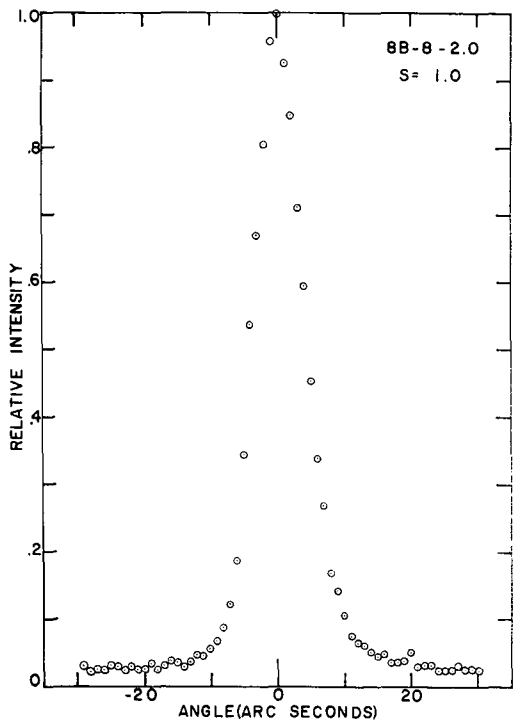

(c) 2.0 Degrees

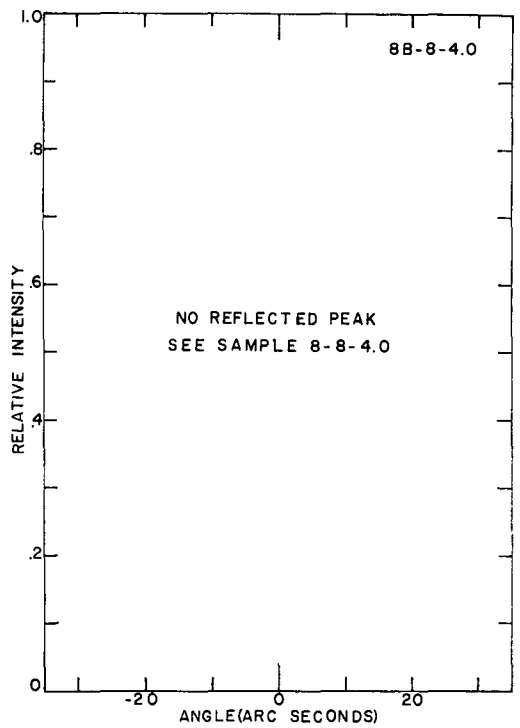

(d) 4.0 Degrees

Figure 11. Sample 8B, 8 Å

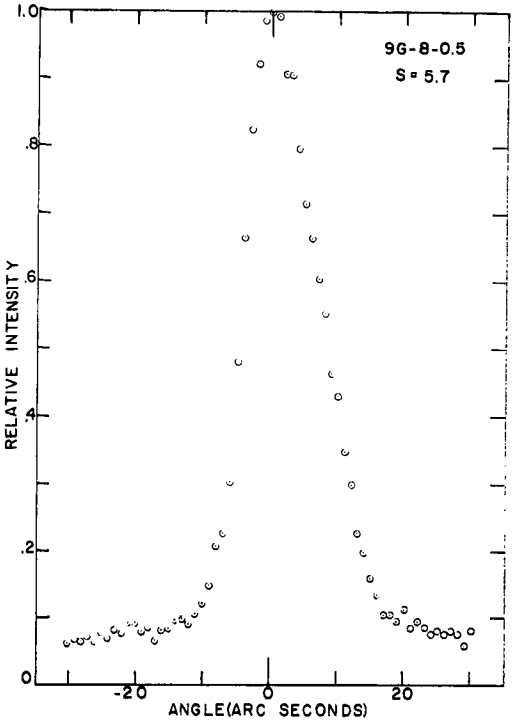

(a) 0.5 Degrees

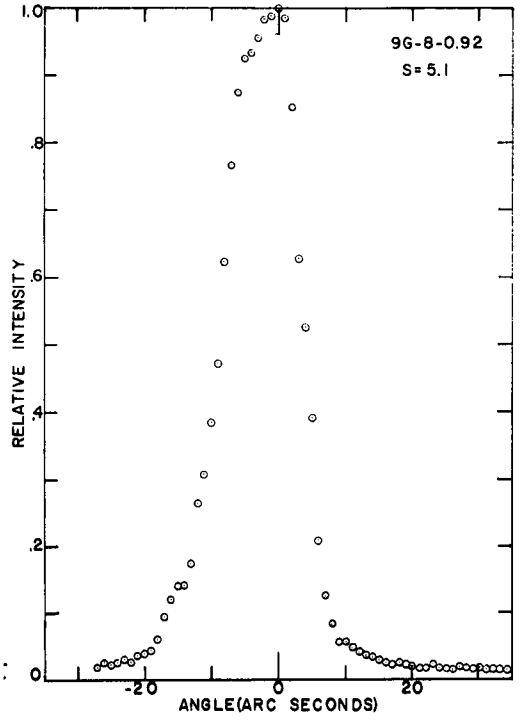

(b) 0.92 Degrees

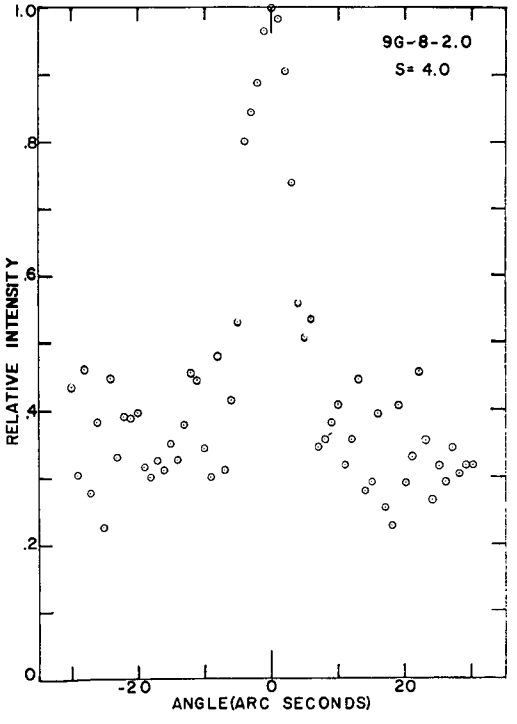

(c) 2.0 Degrees

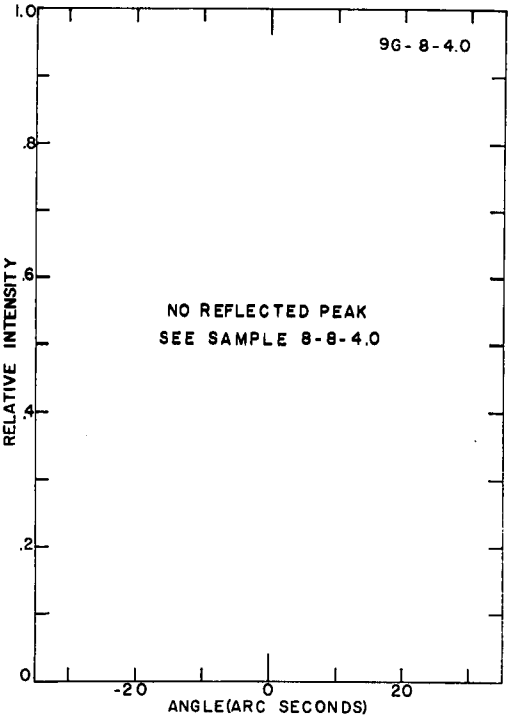

(d) 4.0 Degrees

Figure 12. Sample 9G, 8 Å

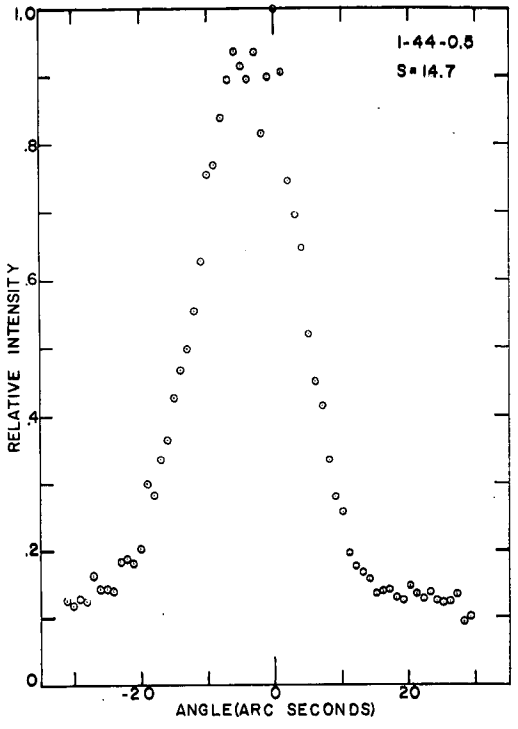

(a) 0.5 Degrees

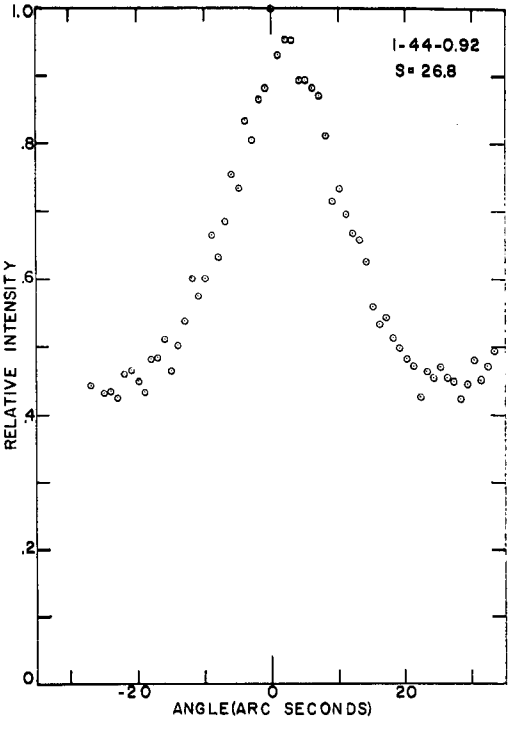

(b) 0.92 Degrees

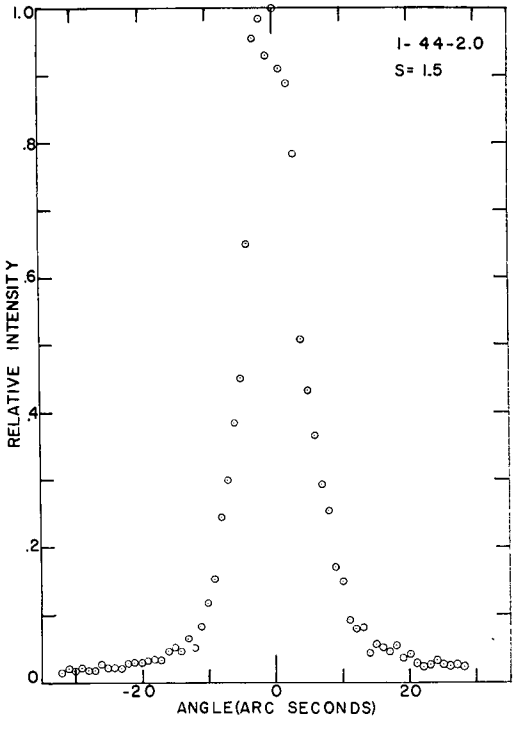

(c) 2.0 Degrees

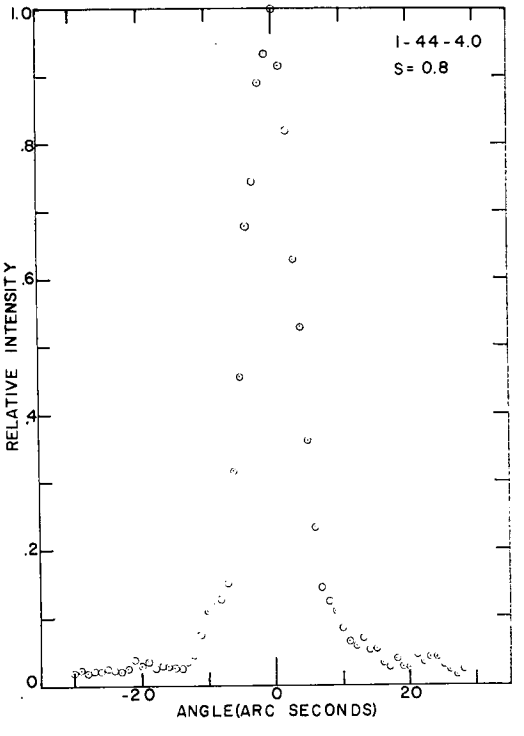

(d) 4.0 Degrees

Figure 13. Sample 1, 44 Å

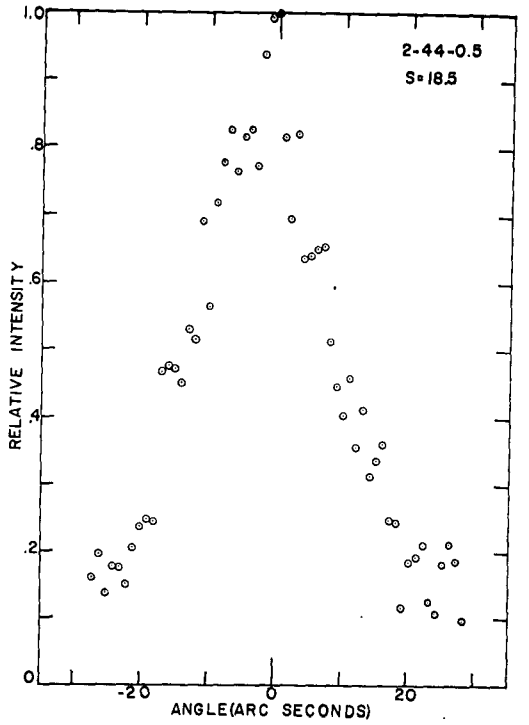

(a) 0.5 Degrees

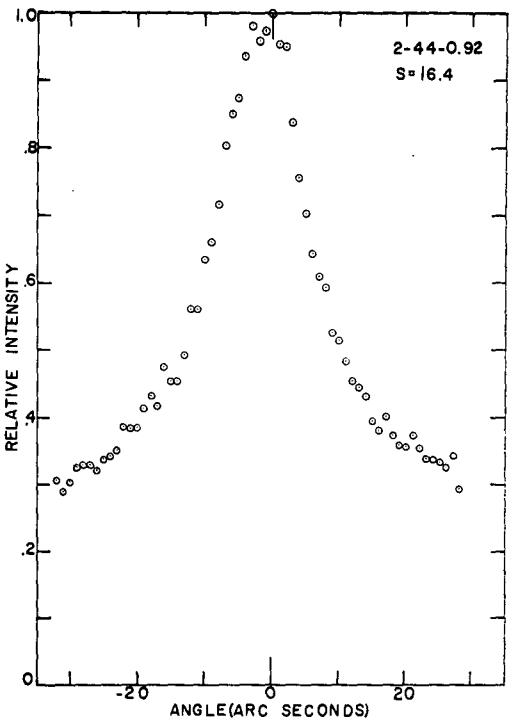

(b) 0.92 Degrees

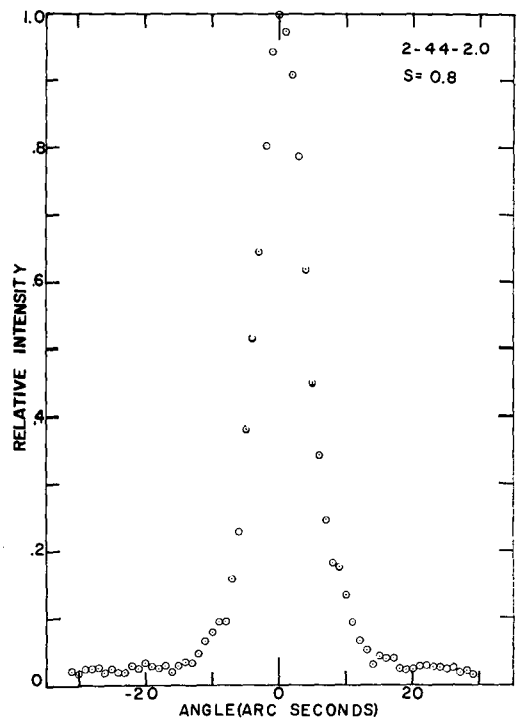

(c) 2.0 Degrees

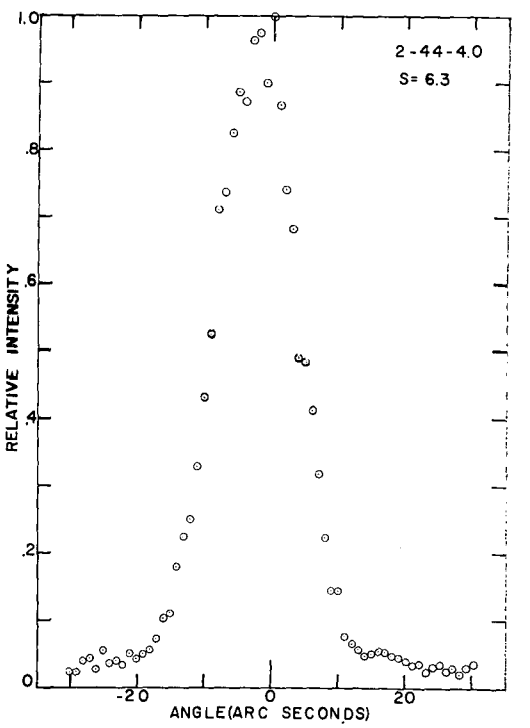

(d) 4.0 Degrees

Figure 14. Sample 2, 44 Å

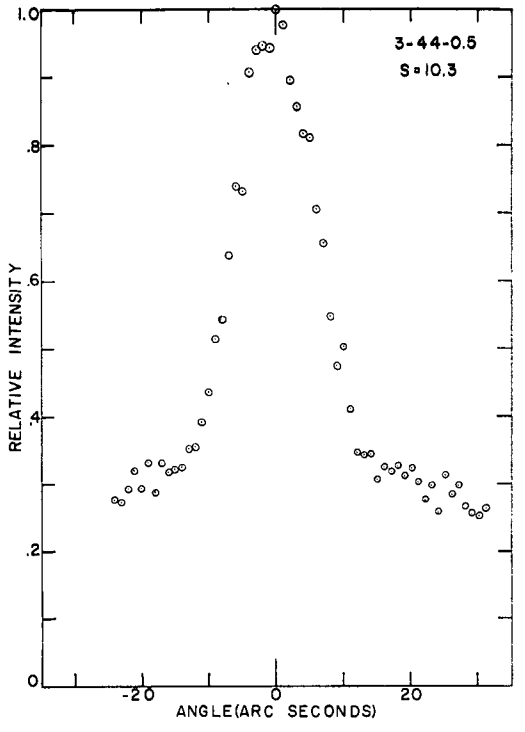

(a) 0.5 Degrees

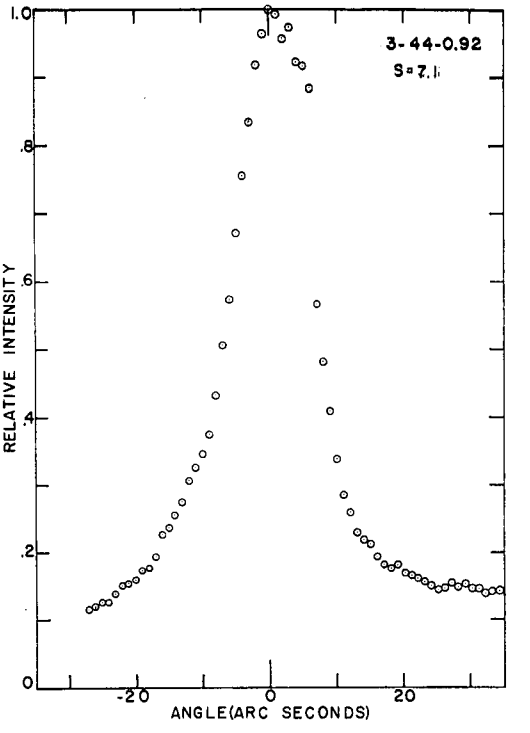

(b) 0.92 Degrees

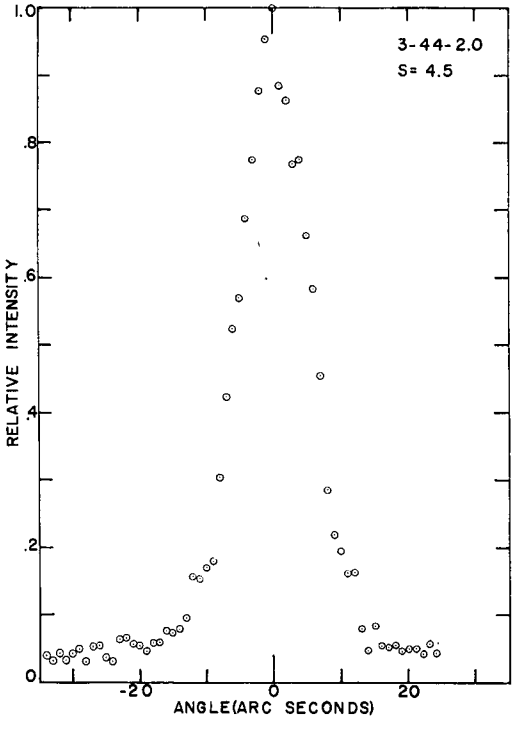

(c) 2.0 Degrees

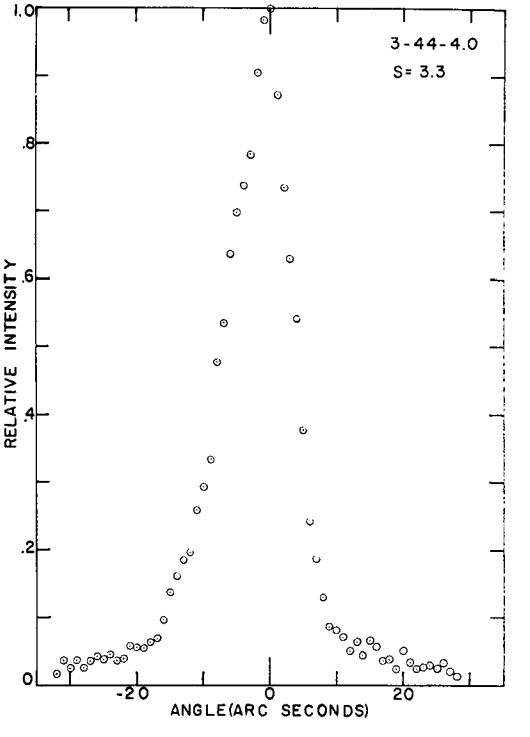

(d) 4.0 Degrees

Figure 15. Sample 3, 44 Å

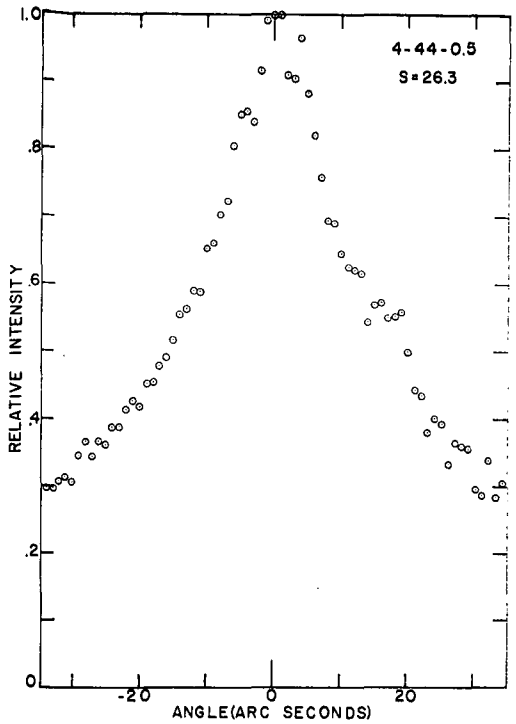

(a) 0.5 Degrees

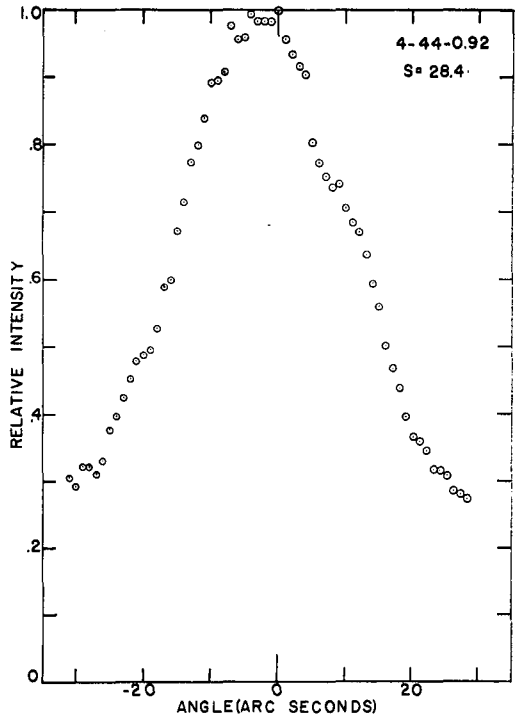

(b) 0.92 Degrees

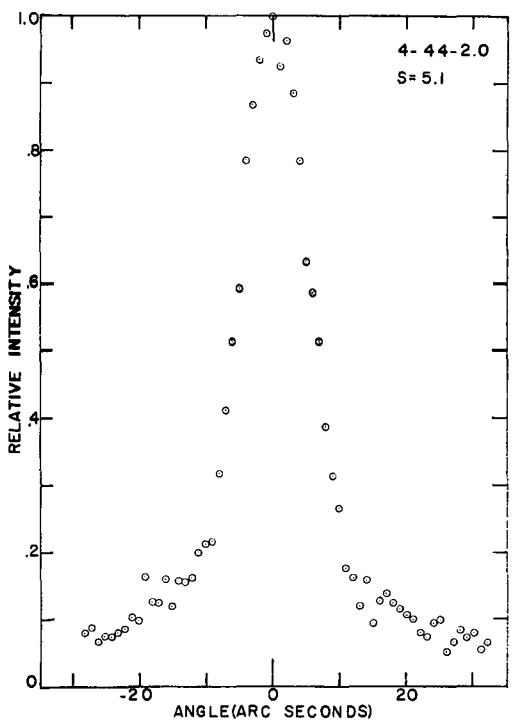

(c) 2.0 Degrees

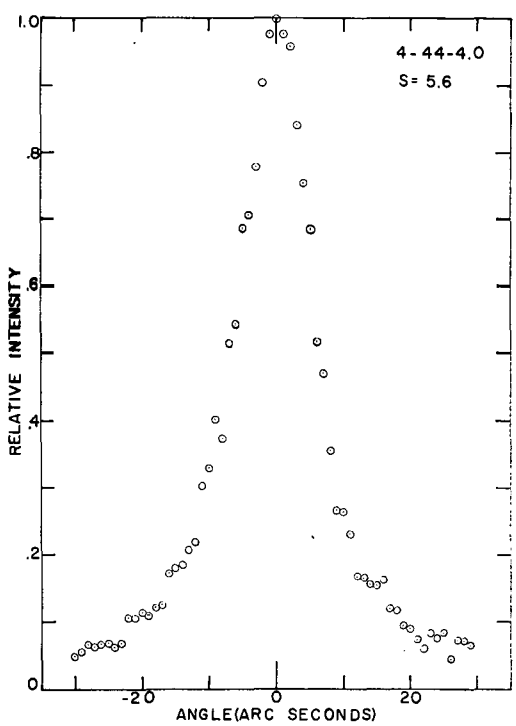

(d) 4.0 Degrees

Figure 16. Sample 4, 44 A

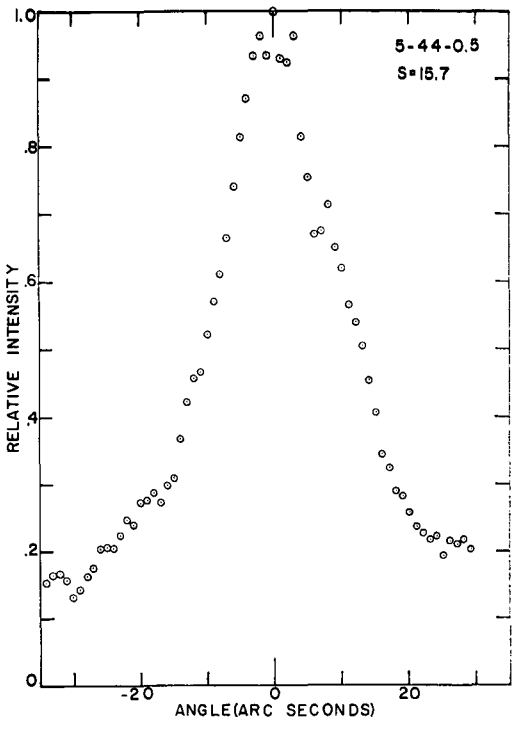

(a) 0.5 Degrees

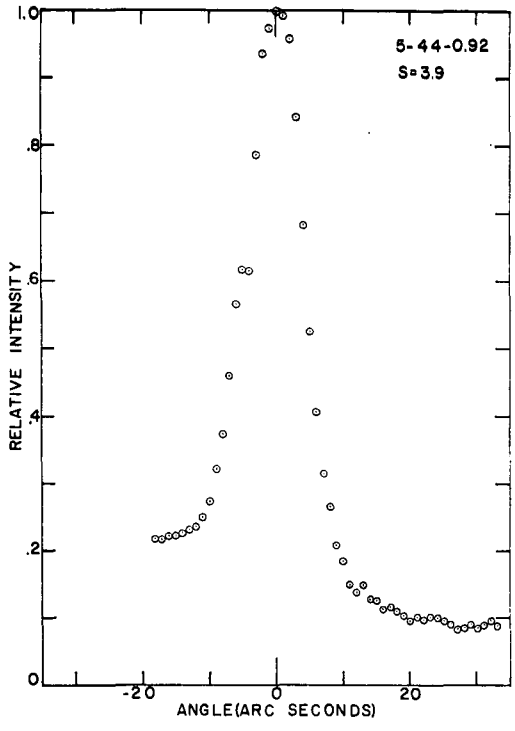

(b) 0.92 Degrees

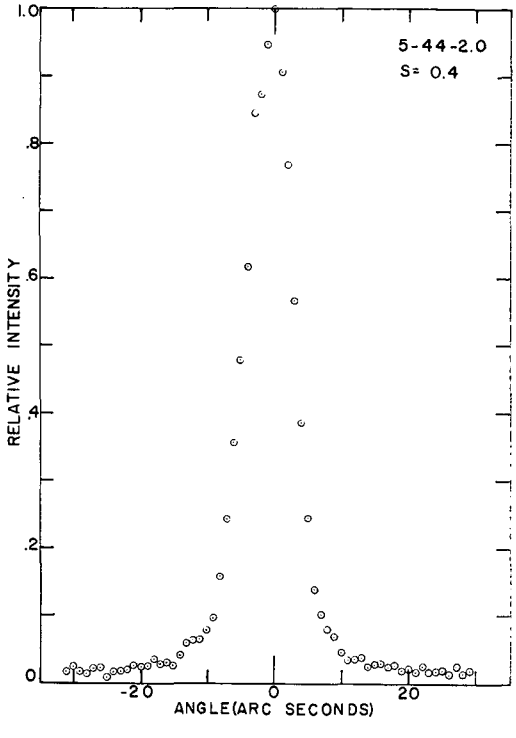

(c) 2.0 Degrees

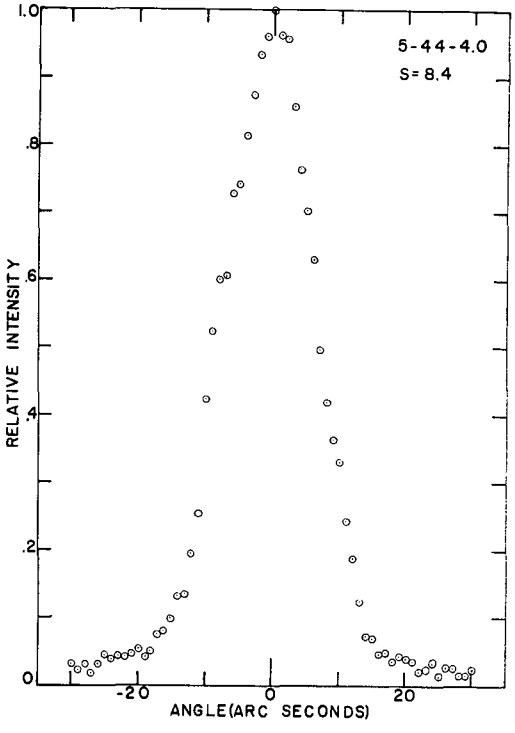

(d) 4.0 Degrees

Figure 17. Sample 5, 44 Å

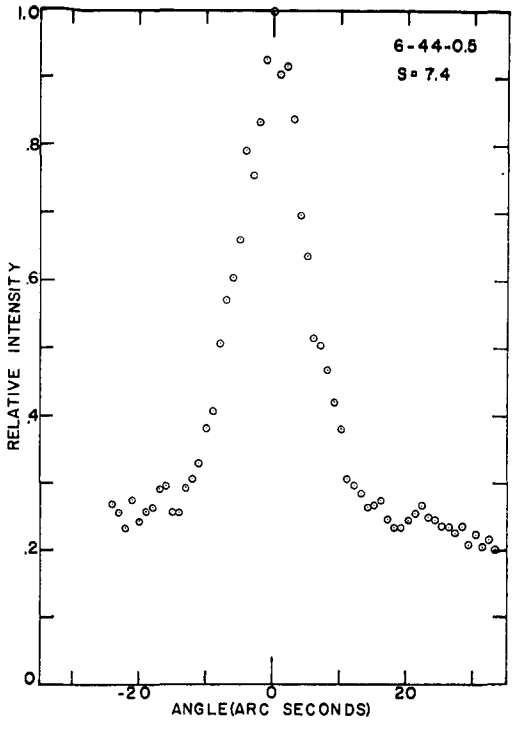

(a) 0.5 Degrees

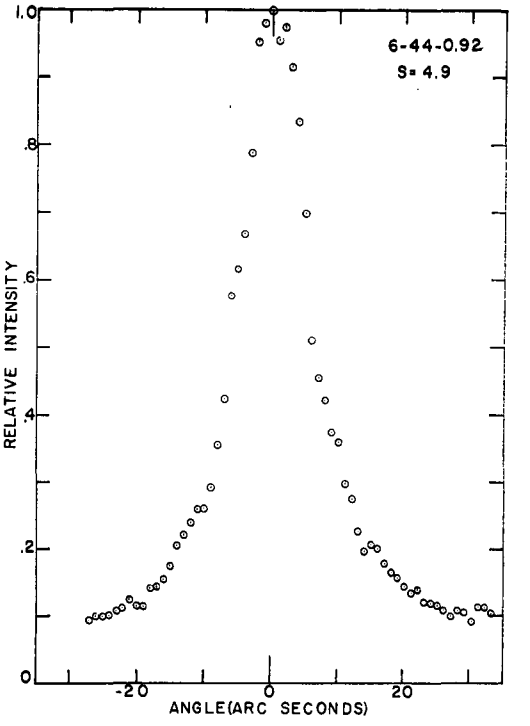

(b) 0.92 Degrees

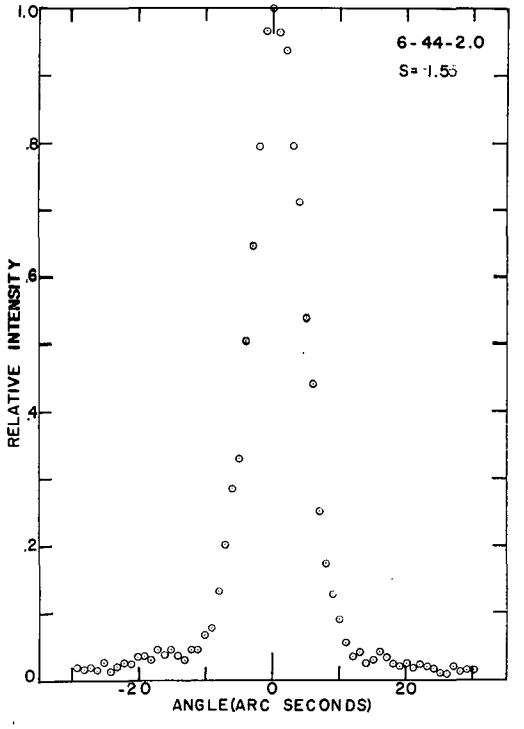

(c) 2.0 Degrees

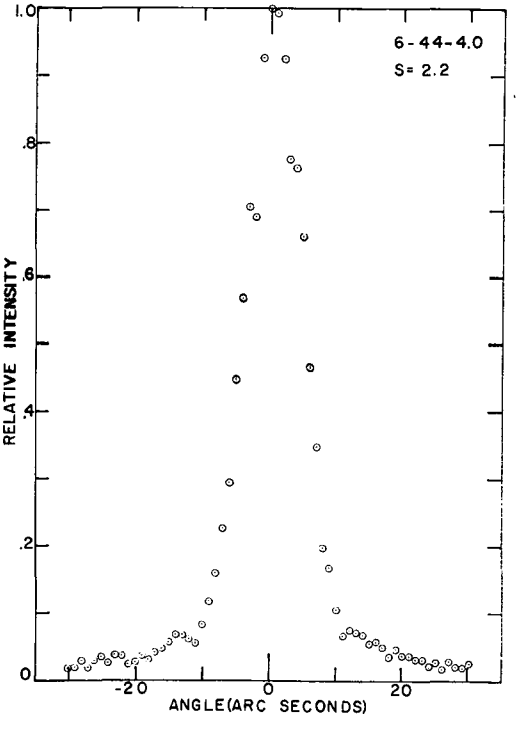

(d) 4.0 Degrees

Figure 18. Sample 6, 44 A

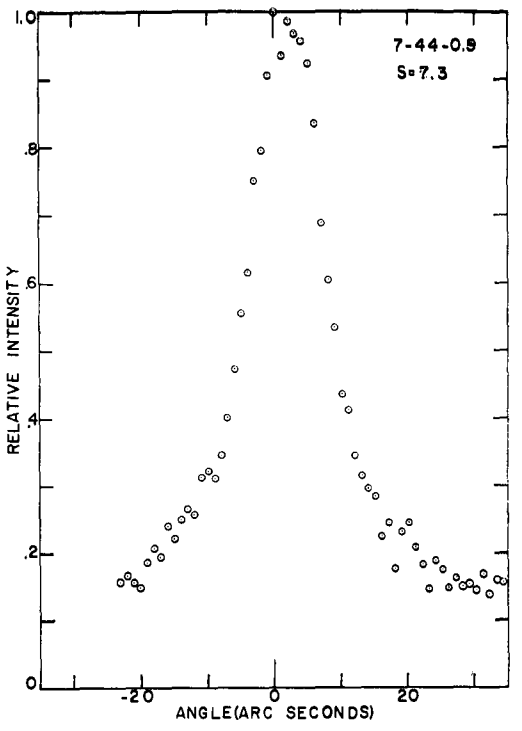

(a) 0.5 Degrees

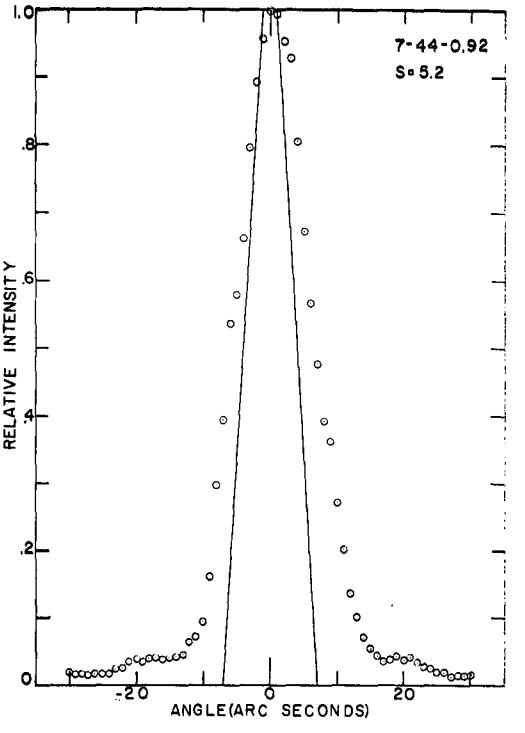

(b) 0.92 Degrees

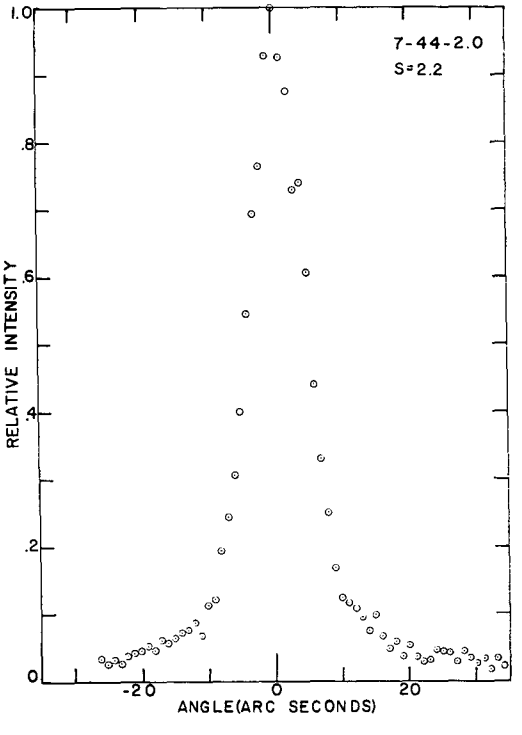

(c) 2.0 Degrees

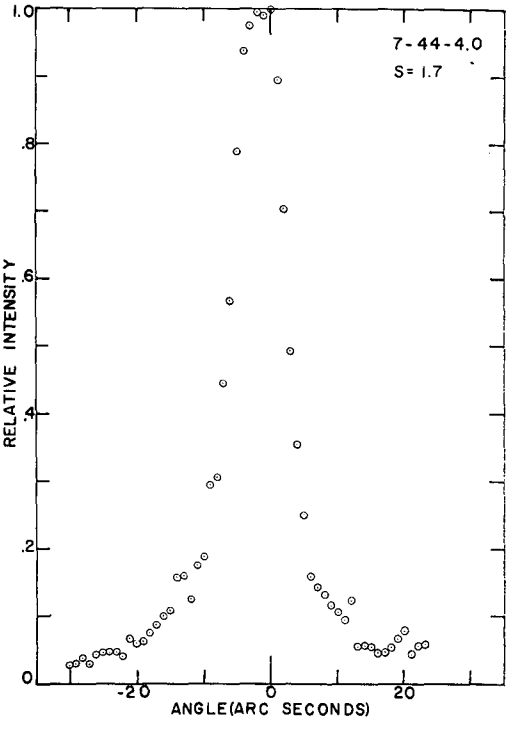

(d) 4.0 Degrees

Figure 19. Sample 7, 44 Å

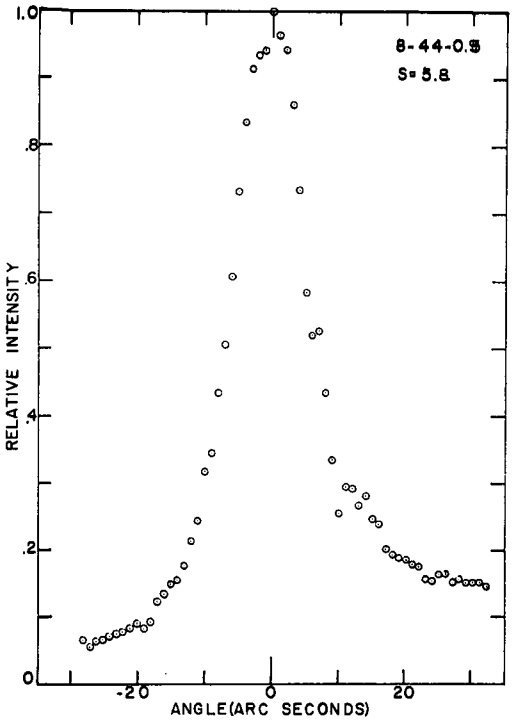

(a) 0.5 Degrees

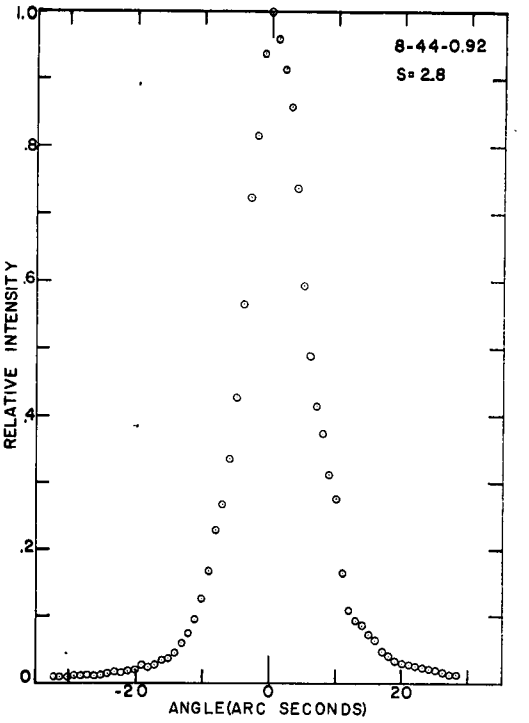

(b) 0.92 Degrees

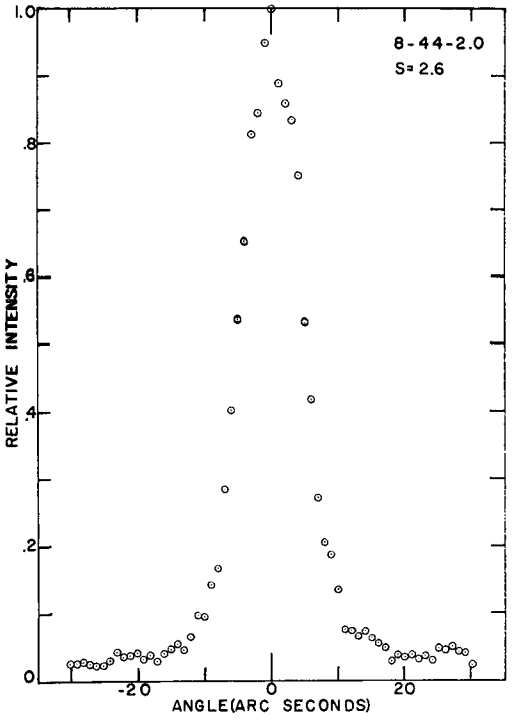

(c) 2.0 Degrees

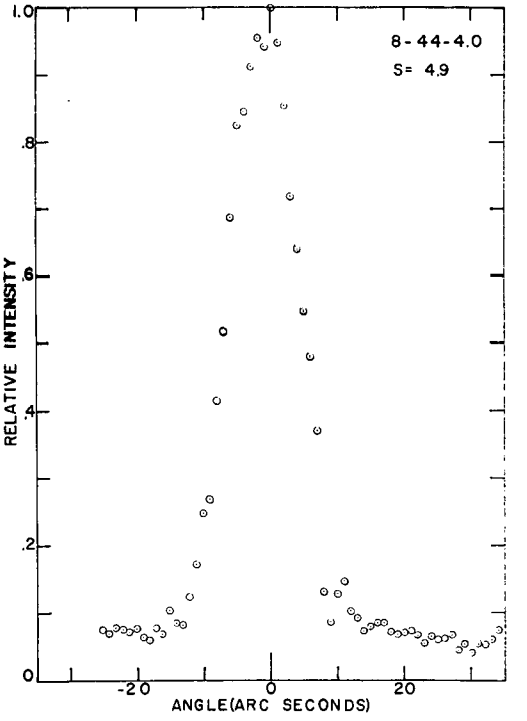

(d) 4.0 Degrees

Figure 20. Sample 8, 44 Å

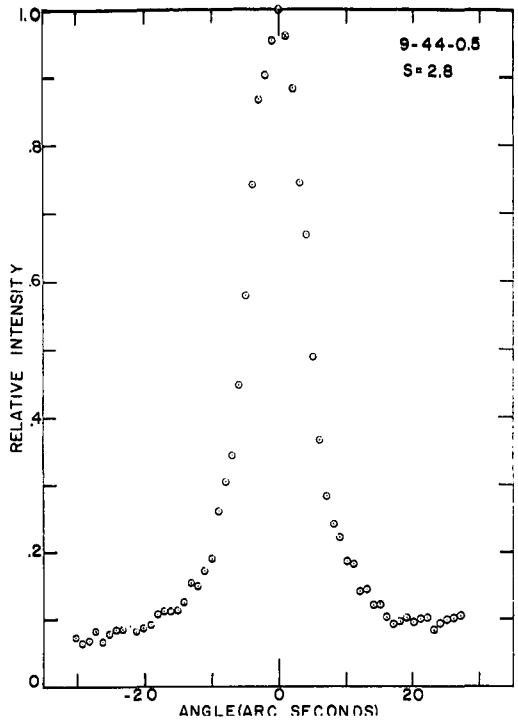

(a) 0.5 Degrees

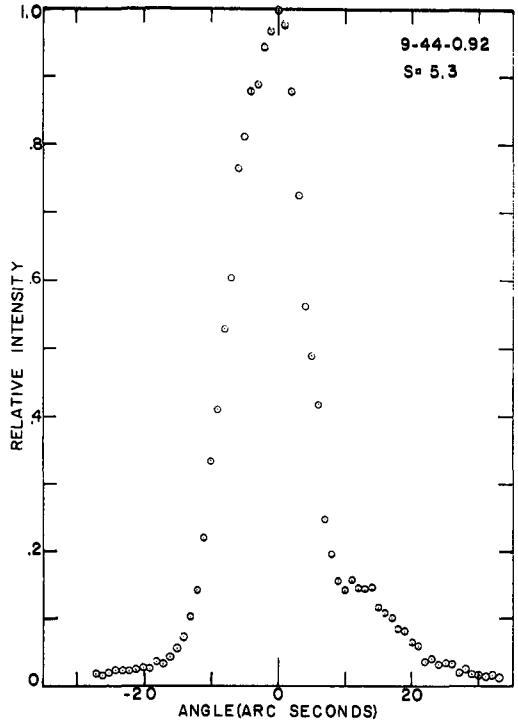

(b) 0.92 Degrees

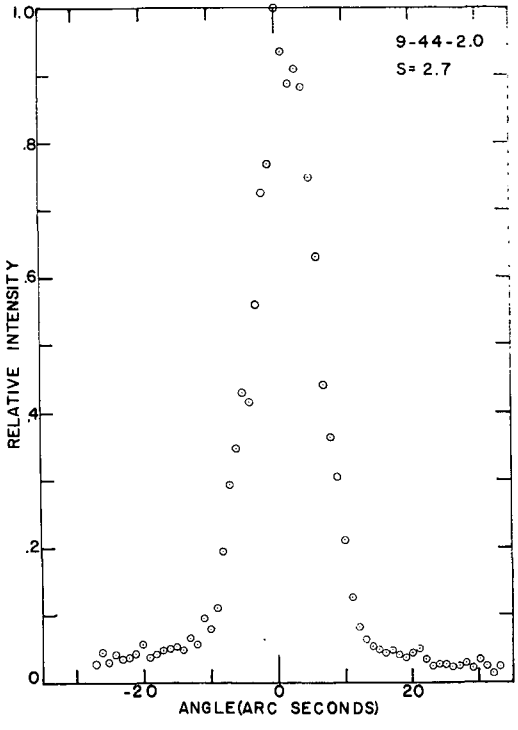

(c) 2.0 Degrees

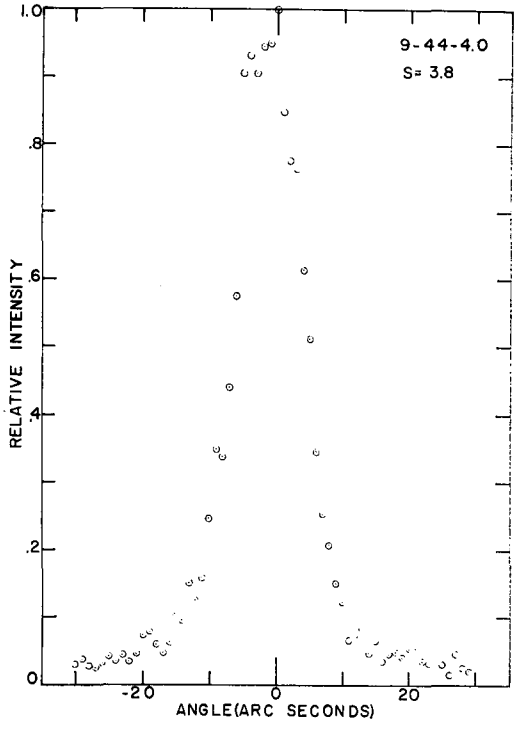

(d) 4.0 Degrees

Figure 21. Sample 9, 44 Å

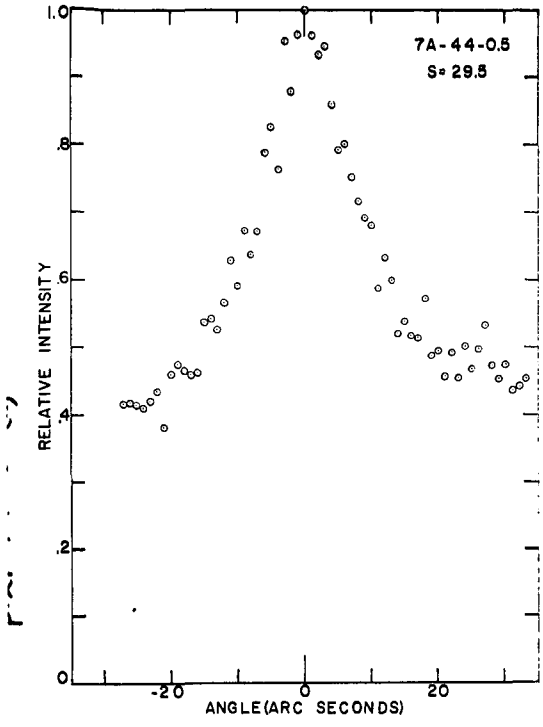

(a) 0.5 Degrees

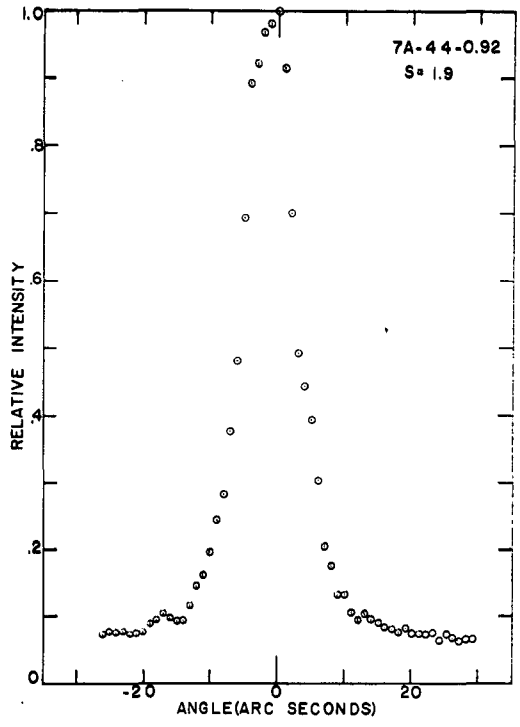

(b) 0.92 Degrees

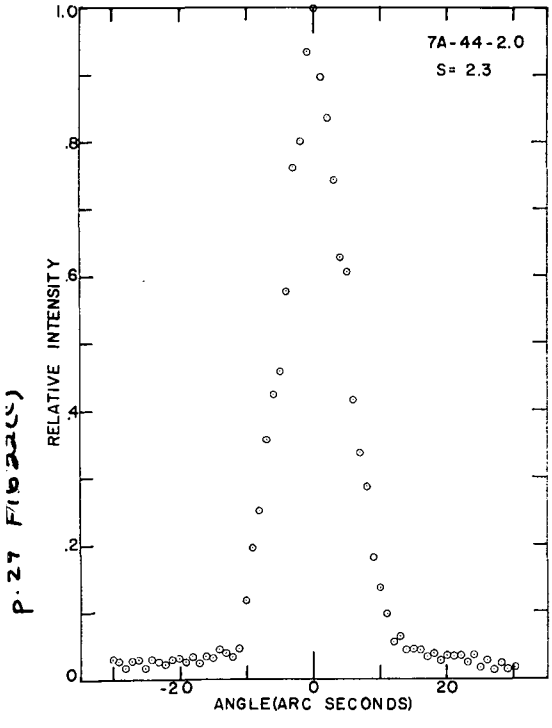

(c) 2.0 Degrees

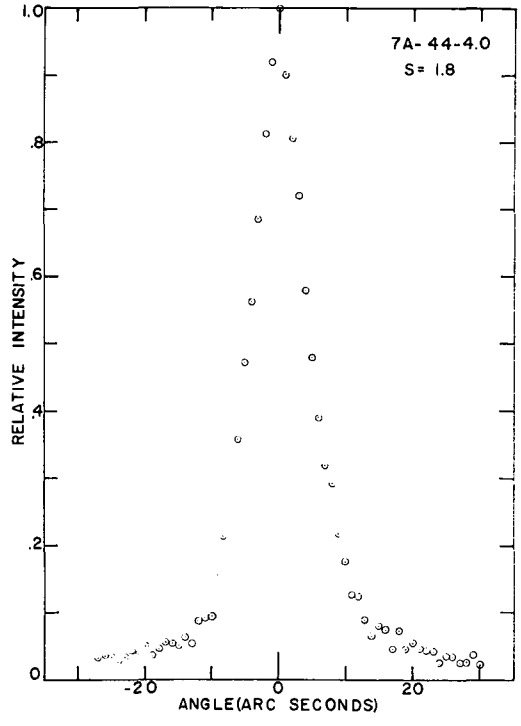

(d) 4.0 Degrees

Figure 22. Sample 7A, 44 Å

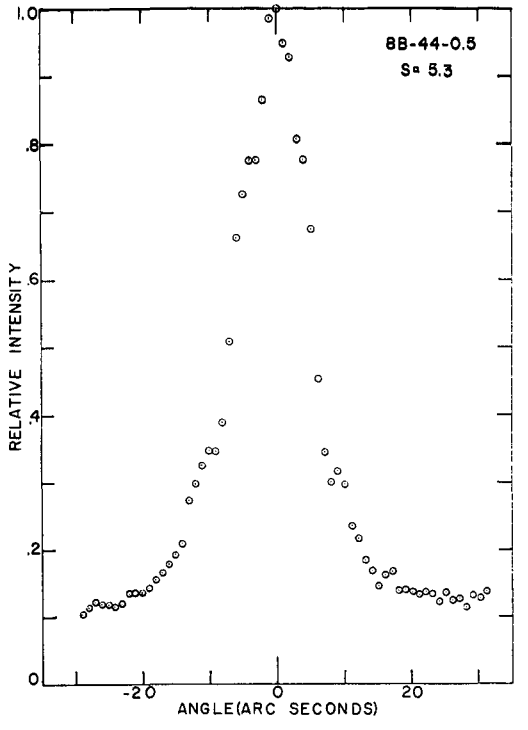

(a) 0.5 Degrees

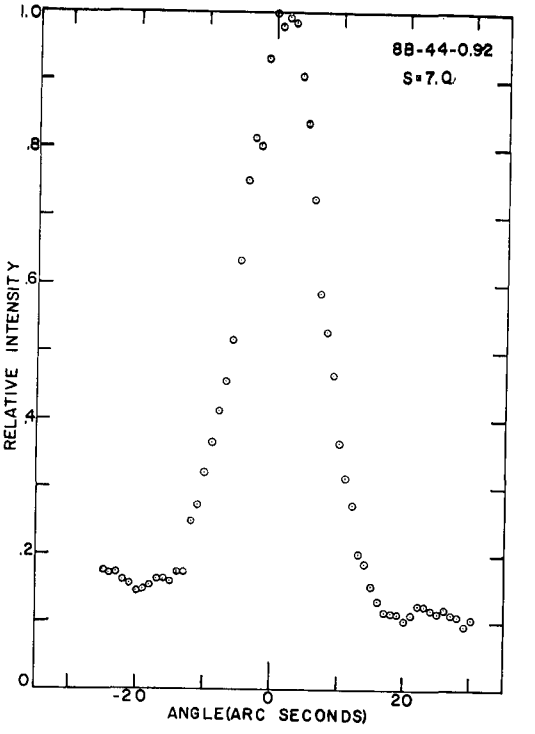

(b) 0.92 Degrees

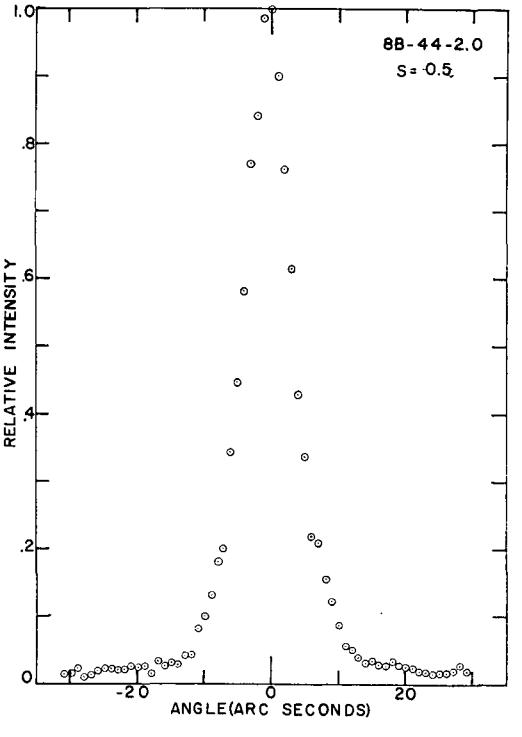

(c) 2.0 Degrees

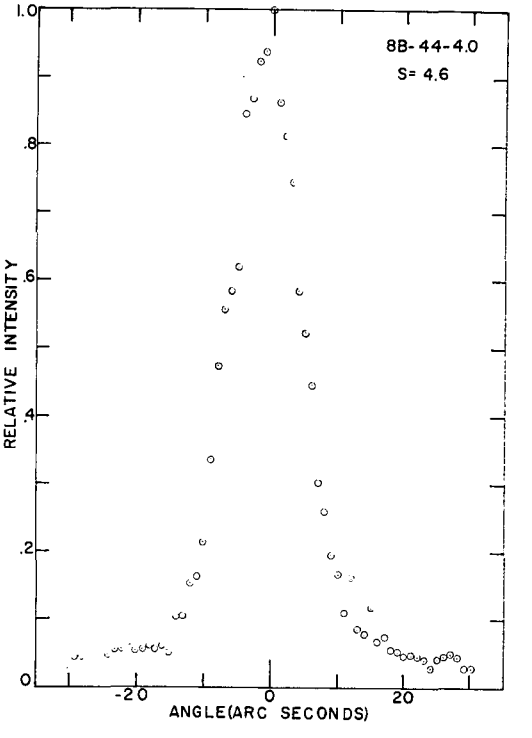

(d) 4.0 Degrees

Figure 23. Sample 8B, 44 Å

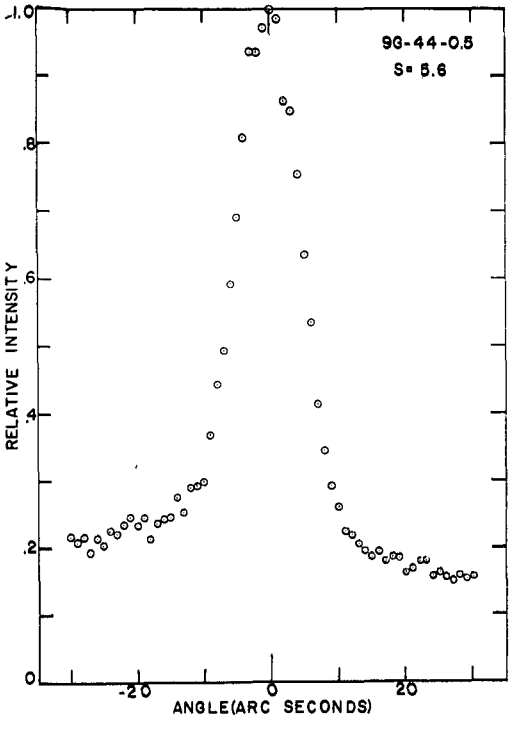

(a) 0.5 Degrees

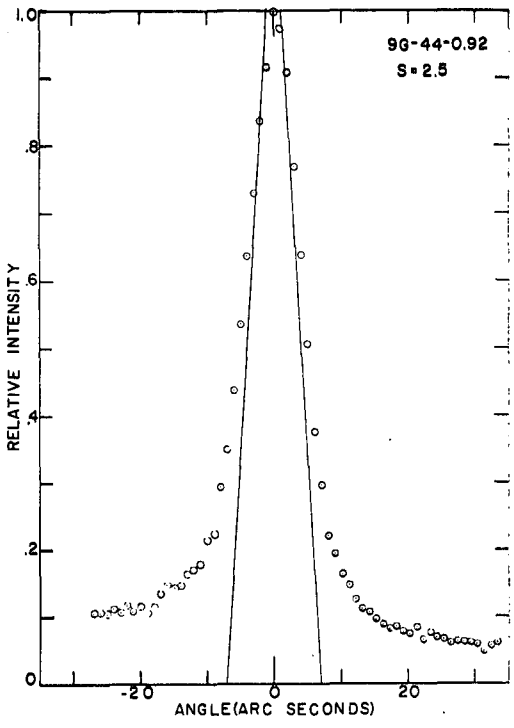

(b) 0.92 Degrees

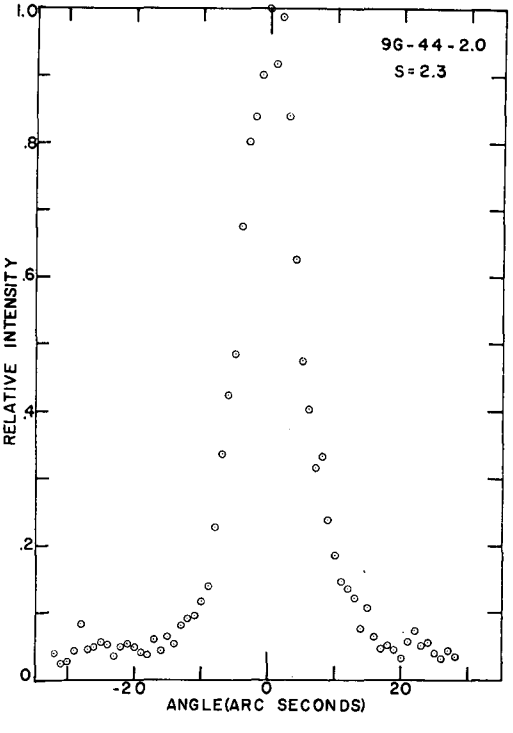

(c) 2.0 Degrees

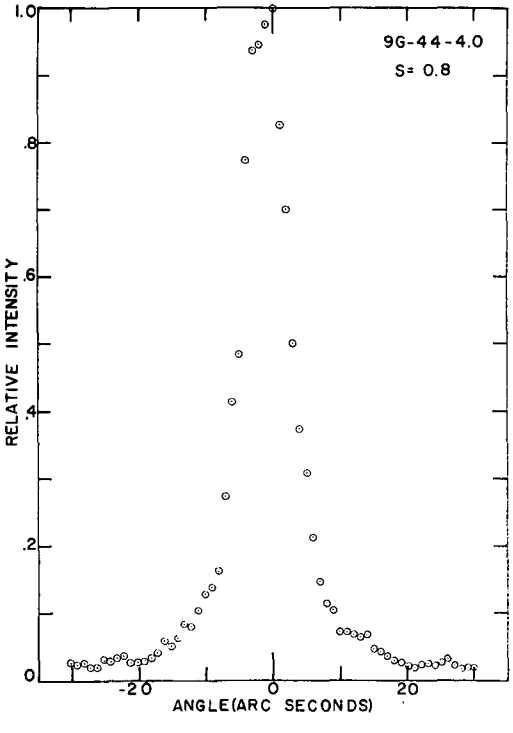

(d) 4.0 Degrees

Figure 24. Sample 9G, 44 A°

The following summarized observations are made for various samples which indicated obvious irregularities.

Sample No. 1 showed irregularities at the peak at 44 Å and 0.92^{o} and 2.0^{o} with considerable deviations at 0.5^{o}. The curves were wide at FWHM for 0.5^{o} (18.7 arc-sec) and extremely wide at 0.92^{o} (34.8 arc-sec). At 8 Å and 0.92^{o} the left side of the curve showed a slight bump. Sample No. 2 was very irregular as well as being wide (22.5 arc-sec) at 44 Å and 0.5^{o}. The curves for Sample No. 4 showed highly irregular peaks at 8 Å and 0.5^{o} and 0.92^{o} (having widths of 23.3 and 25.4 arc-sec, respectively). At 44 Å and 0.92^{o} the curve was very wide (36.4 arc-sec) and also irregular at the peak. The curve for Sample No. 5 at 8 Å and 2.0^{o} indicated it was very irregular at the peak (width of 17.4 arc-sec) while at 44 Å and 0.5^{o} the peak was slightly irregular with a slight peak on the right side. Sample No. 7 at 8 Å and 0.5^{o} showed an extreme irregularity at the peak (width of 27.9 arc-sec) while at 8 Å and 2^{o} the peak was not as bad but showed a bump on the right side (width 27.6 arc-sec). At 44 Å and 0.5^{o} the peak was only slightly irregular.

Nine Points Data

The nine points data was processed so that tables showing relative intensities could be prepared. The intensity values at the nine points were defined as:

I_{-4} = Intensity at -30 arc seconds

I_{-3} = Intensity at -20 arc seconds

I_{-2} = Intensity at -10 arc seconds

I_{-1} = Intensity at -5 arc seconds

I_0 = Intensity at the peak value

I_1 = Intensity at +5 arc seconds

I_2 = Intensity at +10 arc seconds

I_3 = Intensity at +20 arc seconds

I_4 = Intensity at +30 arc seconds

The relative intensity RI was then defined as:

$$RI_j = I_j / I_0$$

This definition produced a set of relative numbers which would then be compared with one another and these values are listed in Tables 1 - 8.

The percent scattered, PS, was defined as:

$$PS = \left\{ \sum_{j=-4}^{4} I_j - \sum_{j=-2}^{2} I_j \right\} \Bigg/ \left\{ \sum_{j=-4}^{4} I_j \right\}$$

This is then another number which can be used as an index of sample performance in comparisons. These values of percent scattered are tabulated in Table 10. The percent scattered values were chosen almost arbitrarily, but do represent an intensity that must come only from scattered radiation. They provide a calculation method which is objective and does not depend on experimental uncertainties in slit width. The method

X-RAY REFLECTANCE OF GODDARD SAMPLES

WAVELENGTH- 8 ANGSTROMS ANGLE OF INCIDENCE .50 DEGREES

ANGLE(ARC SEC)	-30	-20	-10	-5	0	5	10	20	30	
SAMPLE NO.	RELATIVE INTENSITIES									PERCENT SCATTERED
1	.042	.049	.096	.376	1.000	.203	.111	.062	.046	10.05
2	.027	.030	.060	.304	1.000	.360	.059	.028	.024	5.75
3	.028	.034	.039	.246	1.000	.290	.063	.037	.031	7.29
4	.060	.210	1.000	.929	.882	.587	.266	.073	.061	9.94
5	.007	.014	.062	.426	1.000	.262	.046	.015	.012	2.60
6	.004	.010	.035	.326	1.000	.602	.061	.011	.005	1.50
7	.094	.125	.463	.751	1.000	.936	.630	.083	.076	9.10
8	.036	.046	.150	.592	1.000	.570	.169	.047	.040	6.39
9	.133	.146	.211	.439	1.000	.903	.411	.179	.163	17.31
7A	.088	.077	.161	.702	1.000	.343	.102	.084	.080	12.47
8B	.038	.044	.067	.344	1.000	.203	.053	.037	.032	8.33
9G	.094	.107	.305	.735	1.000	.663	.254	.133	.116	13.19

Table 1. Nine Point Data - 8 Angstroms - 0.5 Degrees

X-RAY REFLECTANCE OF GODDARD SAMPLES

WAVELENGTH- 8 ANGSTROMS ANGLE OF INCIDENCE .92 DEGREES

ANGLE(ARC SEC)	-30	-20	-10	-5	0	5	10	20	30	
SAMPLE NO.	RELATIVE INTENSITIES									PERCENT SCATTERED
1	.009	.033	.671	.862	1.000	.567	.042	.011	.008	1.90
2	.003	.021	.044	.466	1.000	.930	.305	.015	.003	1.53
3	.001	.004	.016	.139	1.000	.551	.123	.009	.004	.95
4	.049	.087	.598	.670	1.000	.713	.524	.104	.052	7.69
5	.000	.002	.087	.592	1.000	.198	.014	.001	.000	.23
6	0.	.001	.013	.617	1.000	.649	.123	.002	0.	.11
7	.021	.033	.164	.667	1.000	.543	.135	.030	.019	3.94
8	.004	.011	.051	.463	1.000	.472	.070	.017	.005	1.81
9	.008	.012	.053	.435	1.000	.388	.314	.063	.010	4.11
7A	.005	.016	.108	.392	1.000	.767	.182	.006	.004	1.28
8B	0.	.015	.054	.381	1.000	.286	.019	.001	.002	1.08
9G	.008	.022	.066	.483	.933	1.000	.545	.045	.015	2.87

Table 2. Nine Point Data - 8 Angstroms - 0.92 Degrees

X-RAY REFLECTANCE OF GODDARD SAMPLES

WAVELENGTH- 8 ANGSTROMS ANGLE OF INCIDENCE 2.00 DEGREES

ANGLE(ARC SEC)	-30	-20	-10	-5	0	5	10	20	30	
SAMPLE NO.	RELATIVE INTENSITIES									PERCENT SCATTERED
1	.007	.010	.036	.289	1.000	.236	.027	.008	.012	2.30
2	.019	.030	.056	.487	1.000	.501	.041	.027	.020	4.40
3	.009	.013	.035	.225	1.000	.260	.039	.012	.008	2.67
4	.234	.368	.666	.852	1.000	.436	.241	.222	.166	23.66
5	.022	.021	.748	.686	1.000	.488	0.	0.	.009	1.77
6	0.	.004	.041	.399	1.000	.248	.018	.008	.009	1.16
7	.090	.155	.800	.878	1.000	.773	.578	.145	.084	10.53
8	.056	.066	.096	.281	1.000	.309	.101	.068	.053	11.97
9	0.	.013	.005	.129	1.000	.453	.018	0.	0.	.79
7A	.004	.009	.049	.463	1.000	.318	.059	.006	.002	1.09
8B	.008	.009	.038	.330	1.000	.443	.089	.008	.005	1.61
9G	.146	.088	.010	.298	1.000	.274	.123	0.	0.	12.10

Table 3. Nine Point Data - 8 Angstroms - 2.0 Degrees

X-RAY REFLECTANCE OF GODDARD SAMPLES

WAVELENGTH 8 ANGSTROMS ANGLE OF INCIDENCE 4.00 DEGREES

ANGLE(DEGREES)	-30	-20	-10	-5	0	5	10	20	30	
SAMPLE NO.	RELATIVE INTENSITIES									PERCENT SCATTERED
1	*	*	*	*	*	*	*	*	*	*
2	*	*	*	*	*	*	*	*	*	*
3	*	*	*	*	*	*	*	*	*	*
4	*	*	*	*	*	*	*	*	*	*
5	*	*	*	*	*	*	*	*	*	*
6	*	*	*	*	*	*	*	*	*	*
7	*	*	*	*	*	*	*	*	*	*
8	.602	.347	.505	.453	1.000	.594	.452	.418	.339	36.22
9	*	*	*	*	*	*	*	*	*	*
7A	*	*	*	*	*	*	*	*	*	*
8B	*	*	*	*	*	*	*	*	*	*
9G	*	*	*	*	*	*	*	*	*	*

* NO REFLECTED PEAK

Table 4. Nine Point Data - 8 Angstroms - 4.0 Degrees

X-RAY REFLECTANCE OF GODDARD SAMPLES

WAVELENGTH- 44 ANGSTROMS ANGLE OF INCIDENCE .50 DEGREES

ANGLE(ARC SEC)	-30	-20	-10	-5	0	5	10	20	30	
SAMPLE NO.	RELATIVE INTENSITIES									PERCENT SCATTERED
1	.108	.136	.436	.846	1.000	.650	.285	.141	.074	12.49
2	.200	.432	.891	.995	1.000	.826	.576	.228	.203	19.85
3	.273	.323	.441	.624	1.000	.651	.372	.293	.287	27.58
4	.303	.415	.627	.870	1.000	.733	.610	.350	.285	26.05
5	.150	.204	.404	.667	1.000	.826	.657	.231	.173	17.57
6	.245	.269	.391	.835	1.000	.657	.333	.267	.233	23.98
7	.116	.160	.299	.574	1.000	.502	.267	.149	.131	17.40
8	.052	.089	.435	.684	1.000	.538	.192	.068	.049	8.31
9	.073	.091	.159	.458	1.000	.484	.285	.102	.077	12.58
7A	.316	.332	.482	.748	1.000	.863	.642	.421	.365	27.74
8B	.109	.171	.434	.872	1.000	.491	.288	.184	.163	16.89
9G	.196	.231	.415	.812	1.000	.599	.269	.219	.202	21.52

Table 5. Nine Point Data - 44 Angstroms - 0.5 Degrees

X-RAY REFLECTANCE OF GODDARD SAMPLES

WAVELENGTH- 44 ANGSTROMS ANGLE OF INCIDENCE .92 DEGREES

ANGLE(ARC SEC)	-30	-20	-10	-5	0	5	10	20	30	
SAMPLE NO.	RELATIVE INTENSITIES									PERCENT SCATTERED
1	.304	.444	.491	.873	1.000	.667	.532	.430	.427	31.05
2	.292	.368	.545	.820	1.000	.828	.590	.371	.313	26.22
3	.114	.171	.375	.761	1.000	.889	.284	.165	.145	15.25
4	.299	.458	.834	.987	1.000	.909	.743	.451	.283	25.00
5	.082	.106	.234	.615	1.000	.535	.179	.129	.088	13.63
6	.101	.146	.401	.834	1.000	.526	.223	.114	.092	13.16
7	.015	.030	.106	.498	1.000	.482	.100	.037	.015	4.27
8	.009	.020	.126	.428	1.000	.594	.277	.031	.013	2.89
9	.018	.029	.309	.699	1.000	.467	.156	.040	.018	3.83
7A	.064	.068	.135	.403	1.000	.538	.158	.080	.066	11.11
8B	.132	.146	.307	.637	1.000	.823	.417	.123	.108	13.79
9G	.092	.117	.220	.599	1.000	.565	.183	.089	.071	12.57

Table 6 Nine Point Data - 44 Angstroms - 0.92 Degrees

X-RAY REFLECTANCE OF GODDARD SAMPLES

WAVELENGTH- 44 ANGSTROMS ANGLE OF INCIDENCE 2.00 DEGREES

ANGLE(ARC SEC)	-30	-20	-10	-5	0	5	10	20	30	
SAMPLE NO.	RELATIVE INTENSITIES									PERCENT SCATTERED
1	.005	.020	.042	.296	1.000	.788	.249	.044	.014	3.34
2	.013	.017	.062	.237	1.000	.658	.181	.015	.009	2.48
3	.022	.035	.153	.562	1.000	.654	.179	.029	.022	4.08
4	.069	.120	.332	.936	1.000	.545	.159	.071	.053	9.53
5	.005	.015	.055	.366	1.000	.399	.061	.009	.008	1.93
6	.005	.023	.057	.323	1.000	.535	.081	.015	.004	2.31
7	.025	.035	.212	.985	1.000	.332	.078	.029	.016	3.90
8	.013	.028	.083	.538	1.000	.526	.123	.023	.005	2.95
9	.009	.036	.312	.796	1.000	.390	.057	.016	.014	2.86
7A	.020	.021	.108	.454	1.000	.604	.128	.026	.006	3.09
8B	.009	.022	.078	.344	1.000	.431	.118	.022	.012	3.18
9G	.013	.026	.225	.792	1.000	.594	.206	.031	.015	2.94

Table 7. Nine Point Data - 44 Angstroms - 2.0 Degrees

X-RAY REFLECTANCE OF GODDARD SAMPLES

WAVELENGTH- 44 ANGSTROMS ANGLE OF INCIDENCE 4.00 DEGREES

ANGLE(ARC SEC)	-30	-20	-10	-5	0	5	10	20	30	
SAMPLE NO.	RELATIVE INTENSITIES									PERCENT SCATTERED
1	.009	.017	.040	.159	1.000	.702	.126	.029	.013	3.26
2	.009	.029	.424	.887	1.000	.478	.134	.028	.021	2.90
3	.008	.042	.283	.694	1.000	.370	.069	.037	.000	3.53
4	.061	.095	.303	.553	1.000	.777	.263	.083	.056	9.26
5	.020	.043	.414	.739	1.000	.699	.322	.029	.014	3.25
6	.004	.016	.070	.441	1.000	.657	.094	.024	.012	2.42
7	.017	.033	.118	.442	1.000	.490	.049	.024	.012	3.94
8	.030	.058	.235	.822	1.000	.539	.112	.054	.022	5.70
9	.014	.031	.151	.598	1.000	.641	.143	.025	.004	2.82
7A	.013	.036	.081	.465	1.000	.439	.083	.028	.015	4.22
8B	.010	.037	.199	.613	1.000	.517	.153	.034	.015	3.73
9G	.012	.014	.117	.477	1.000	.300	.061	.009	.005	2.02

Table 8. Nine Point Data - 44 Angstroms - 4.0 Degrees

of adding the area under the curve is subject to large uncertainties because of possible slit width errors.

Reflecting Efficiency Measurements

The efficiency of reflection can not be determined absolutely with this measurement system because of variables in the source geometry and the location of the secondary counter. These factors cannot be controlled with sufficient accuracy to permit a calibration by means of a known sample (if one exists). Perhaps later measurements can be done in this way, but equipment modifications must be made first. The "efficiency factor", see Table 11, is not an attempt at measuring reflecting efficiency, but, rather, is used to normalize the data against fluctuations in source intensity. The secondary detector records an intensity value (not flux) simultaneously with that obtained in the primary detector. The values recorded will vary as source output varies, but their ratio will not vary (neglecting counting statistics). Thus, the shape of the curves is not influenced by fluctuations in the source intensity, but the absolute reflecting efficiency is not measured. This number can be used, however, to give some insight into the location of critical angles in reflecting efficiency.

For convenience in comparing the results, Tables 9, 10, and 11 contain compilations of the scattering widths, percent scattered, and the efficiency factor, respectively.

WAVELENGTH(ANGSTROMS)	8				44			
ANGLE(DEGREES)	0.5	0.92	2.0	4.0	0.5	0.92	2.0	4.0
SAMPLE	SCATTERING WIDTH (ARC SEC.)							
1	-0.2	9.4	-1.2	*	14.7	26.8	1.5	0.8
2	2.5	9.9	1.2	*	18.5	16.4	0.8	6.3
3	3.5	4.3	-0.4	*	10.3	7.1	4.5	3.3
4	19.6	17.4	10.3	*	26.3	28.4	5.1	5.6
5	4.5	4.6	9.4	*	15.7	3.9	0.4	8.4
6	4.3	8.8	-1.2	*	7.4	4.9	1.5	2.2
7	11.4	4.2	19.6	*	7.3	5.2	2.2	1.7
8	4.5	4.0	-1.3	*	5.8	2.8	2.6	4.9
9	3.5	-0.2	-1.5	*	2.8	5.3	2.7	3.8
7A	-1.0	3.1	1.8	*	29.5	1.9	2.3	1.8
8B	-0.8	0.1	1.0	*	5.3	7.0	0.5	4.6
9G	5.7	5.1	4.0	*	5.6	2.5	2.3	0.8

NO REFLECTED PEAK

Table 9. Compilation of Scattering Width Data

WAVELENGTH (ANGSTROMS)	8				44			
ANGLE(DEGREES)	0.5	0.92	2.0	4.0	0.5	0.92	2.0	4.0
SAMPLE	PERCENT SCATTERED							
1	10.05	1.90	2.30	*	12.49	31.05	3.34	3.26
2	5.75	1.53	4.40	*	19.85	26.22	2.48	2.90
3	7.29	.95	2.67	*	27.58	15.25	4.08	3.53
4	9.94	7.69	23.66	*	26.05	25.00	9.53	9.26
5	2.60	.23	1.77	*	17.57	13.63	1.93	3.25
6	1.50	.11	1.16	*	23.98	13.16	2.31	2.42
7	9.10	3.94	10.53	*	17.40	4.27	3.90	3.94
8	6.39	1.81	11.97	36.22	8.31	2.89	2.95	5.70
9	17.31	4.11	.79	*	12.58	3.83	2.86	2.82
7A	12.47	1.28	1.09	*	27.74	11.11	3.09	4.22
8B	8.33	1.08	1.61	*	16.89	13.79	3.18	3.73
9G	13.19	2.87	12.10	*	21.52	12.57	2.94	2.02

*NO REFLECTED PEAK

Table 10 - Compilation of Percent Scattered Data

WAVELENGTH(ANGSTROMS)	8				44			
ANGLE(DEGREES)	0.5	0.92	2.0	4.0	0.5	0.92	2.0	4.0
SAMPLE	EFFICIENCY FACTOR							
1	.03892	.07357	.00050	*	.01600	.02300	.01424	.00745
2	.02578	.02773	.00066	*	.00514	.05515	.01396	.00594
3	.03126	.03720	.00035	*	.37834	.23303	.00600	.00504
4	.02310	.00069	.00018	*	.20647	.05265	.00919	.00316
5	.01783	.05264	.00008	*	.03616	.06642	.01478	.00777
6	.02750	.05567	.00010	*	.19941	.09198	.01522	.00518
7	.00213	.00365	.00205	*	.03148	.14327	.01655	.01307
8	.00704	.00367	.00034	.00005	.06215	.25202	.01061	.00358
9	.00156	.00591	.00010	*	.07049	.04246	.02896	.00545
7A	.00282	.00097	.00069	*	.01937	.08710	.01164	.00586
8B	.01900	.01213	.00056	*	.06274	.03128	.01953	.00616
9G	.00106	.00582	.00003	*	.03243	.04996	.00509	.00630

NO REFLECTED PEAK

Table 11. Compilation of Efficiency Factors

Statistical Considerations

There was no statistical requirement with respect to intensity in the case of the 61 point scattering curves. These were used to determine the location of the peak for the more accurate nine points data. The time interval was fixed at 100 seconds, and the number of counts collected in this period was used. The intensity varied somewhat because of several factors, but an average peak intensity was about 2500 counts with points away from the peak proportionally lower.

The nine points data were taken so that the number of counts at the peak was greater than 10,000 for one angle of incidence. The other points for that sample at that wavelength were then recorded for an equal amount of time. These times ranged from 100 sec for some samples to 800 sec for others. The times used in each case were:

Sample	Time for Nine Points Data 8 Å	44 Å
1	600 sec	800 sec
2	250 sec	300 sec
3	400 sec	100 sec
4	400 sec	300 sec
5	300 sec	400 sec
6	400 sec	200 sec
7	200 sec	200 sec
8	400 sec	100 sec
9	200 sec	400 sec
7A	500 sec	500 sec
8B	300 sec	400 sec
9G	200 sec	400 sec

The uncertainty in the values of percent scattered collected in Table 10 is about ± 0.2.

Illuminated Area of Sample

The height of the beam is limited by the height of the source which is small (approximately .010") and the height of the entrance to the detector (½"). The height of the illuminate area is about ¼" since the shims were placed well outside this limit and only those rays reflected at the right height to enter the detector slit were counted. The width of the illuminated area is given by the equation $W = 2h/\tan\theta$, where h is the slit spacing at the sample and θ is the glancing angle of incidence. For the experimental conditions then, the illuminated areas are given by:

Height = 0.25"		Width	
	θ	h = .001"	h = .002"
	0.5°	W = .229"	W = .458"
	0.92°	W = .124"	W = .249"
	2.0°	W = .057"	W = .114"
	4.0°	W = .029"	W = .057"

The error in θ is $\pm$2 arc minutes.

Samples Used in Measurements

Twelve government furnished samples were tested in this study. These were numbered 1, 2, 3, 4, 5, 6, 7, 8, 9, 7A, 8B, and 9G. Samples 1, 2, and 3 were the first samples to be furnished and they are metal - probably Kanigen coated aluminum. Samples 4, 5, and 6 arrived in the second group. Number 4 was a metal sample which was cleaned by Dr. Underwood and may have

been damaged. Sample 5 was an amber colored glass of about one inch thickness - probably Cer-Vit. Sample 6 was a clear glass of about one inch thickness - the shipping container was labeled ULE. Sample 7 was a small metal sample of 1½ inches diameter which had a mounting screw hole tapped in the rear face. Sample 8 was a metal sample that had a protective coating on the surface. The coating was removed, but a stain was evident on the surface of the sample. Sample 9 was an amber colored glass about ½ inch thick - probably Cer-Vit also. Samples 7A, 8B, and 9G were supplied by P. W. Sanford of UCL and were identified as A, B, and G by him. The three were all metal samples. We did not know the details of manufacture or even the manufacturer of the samples in order that there be no question about objectivity.

Some irregularities were observed in the physical appearance of samples. These were:

Sample No. 1 - good polished surface, no irregularities.

Sample No. 2 - good polished surface, no irregularities.

Sample No. 3 - Appeared to have surface pits.

Sample No. 4 - Appeared to have surface pits with a very slightly discolored area (about ½ in. dia.).

Sample No. 5 - good polished surface, no irregularities.

Sample No. 6 - good polished surface, no irregularities.

Sample No. 7 - Appeared to have surface pits.

Sample No. 8 - sample discolored over most of surface, but badly discolored over 1/3 area (looks like some coating remained on).

Sample No. 9 - good polished surface, no irregularities.

Sample No. 7A - appeared to have surface pits.

Sample No. 8B - surface has milky film as if solvent used to clean surface left some streaks.

Sample No. 9G - polished surface appeared to have some surface pits.

Telescope Mirror Tests

A Kanigen coated beryllium mirror was tested in the long vacuum line in the same way that three quartz mirrors had been tested previously. This test produced results which were compared with other performance data. Relative performance of this mirror was substantially poorer than that of the other three telescopes tested.

Resolution Studies

One X-ray source and one visible light source were used in these tests. The visible light source made use of the filaments of the X-ray source. A ground glass screen was placed between the filaments and the resolution chart so as to diffuse the light. The spectral content of the visible light source was essentially continous tungsten radiation (white light). The

8.34 Å aluminum source was essentially monochromatic with only small contributions from 8 Å K_β radiation and 6.94 Å tungsten radiation.

The X-ray photographs taken with the Kanigen coated beryllium mirror used a twelve-wire filament configuration which produced uniform X-ray intensity in the source.

Three resolution charts were used in these tests. A Buckbee-Mears X-ray resolution chart was used for data runs 61-65, 70, and 71. This chart had three bar sets of 5, 7.5, and 10 arc seconds angular resolution. Also placed on the chart were three dots of 5, 2, 1 arc seconds angular extent. For data runs 66-69, and 72, a set of three horizontal bars of 30 arc seconds angular resolution was used. For data run 73, a chart consisting of one pinhole of 20 arc seconds angular resolution was used.

Three types of film were used in these tests. Film type SO-212 was used for data runs 61-67, 71, and 73. This film was developed in Kodak D-19 at 68°F for 8 minutes, washed in distilled water for 30 seconds (to remove jet backing), stop bath was for 30 seconds, and fixed in Kodak Rapid Fixer for 2½ minutes. A 30-minute rinse was followed by a photo-flow solution and the film was then dried. At the start of the 30-minute rinse, it was necessary to apply light rubbing to the film to remove the jet backing not removed during the 30 second wash in distilled

water. Film type 103-0 was used for data run 68 and film type 103-AO was used for data runs 69, 70, and 72. Type 103-O and type 103-AO were developed in Kodak D-19 at 68°F for 5 minutes and for 4 minutes, respectively, with the rest of the processing being the same as for type SO-212. In spite of careful handling, numerous flaws were present in the exposed film strips. This is thought to be caused by the camera mechanism. The exposures were cut and mounted in 2-inch by 2-inch slide holders to protec the photographs. Each slide has a label giving the run and exposure number, the wavelength, the relative distance, the azimuth angle ϕ, and the elevation angle θ. When the slide is held so that the label is in the left hand corner, the photograph has the same orientation as if the observer were viewing the image in a ground glass screen attached to the telescope.

The telescope assembly (Government furnished property) was placed in the test chamber. The test chamber and 200-foot line were evacuated. The pressure was reduced to 7.8×10^{-6} Torr (average of 13 runs) as measured by an ion gauge which was placed in close proximity to the S056 beryllium mirror. Exposures of the test pattern (Buckbee-Mears, pinhole, or 30 arc-second bar set) were then made using the camera which was provided with the telescope assembly.

The graph shown in Figure 25 was obtained by visual inspection. All observers have commented on the subjectivity of the

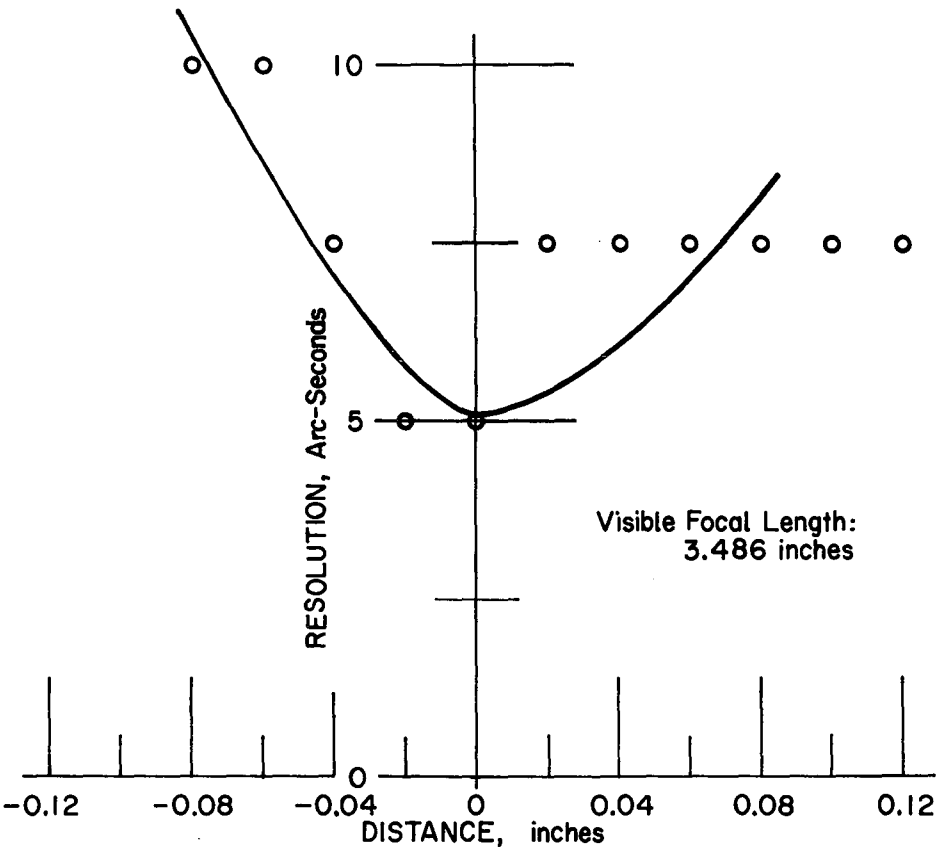

Figure 25 - Resolution Curve

inspection technique which was a hand magnifier. From past experience with previous telescope test data (see references 1, 2, and 3), this method was found superior to other optical aids in analyzing the test data.

For all the visible runs, the anode voltage and current were zero. For the 8 Å (aluminum) runs, the anode voltage was 6.0 KV and the anode current was 50 ma. All other pertinent information concerning the exposures is given in Table 12. Since many of the frames were under-exposed, only the exposures that are readable are listed in Table 12.

Point Source Tests

One method of testing an X-ray telescope is to produce a point source of X-rays and see how well the telescope recreates the image of the source. By comparing the number of X-rays counted at the center of the image to the number of X-rays entering the telescope, the reflection efficiency can be obtained. An indication of the telescope's scattering properties can be obtained by measuring the X-radiation which is reflected away from the main beam.

An arrangement having a 0.010" pinhole ($\sim$ 28 arc-sec) was positioned centrally in the focal plane fixture at the rear of the telescope with a flow proportional counter placed behind the pinhole. The pinhole arrangement could be positioned 10 arc

Data Run Frame	Ex-pos. No.	Adjustable Housing Position (Inches)	ϑ (Arc-Min)	ϕ (Arc-Min)	Filter Material	Source	Exposure Unit	Film Type
63-1	1	3.606	0	0	Blank	Vis	.70 seconds	SO-212
63-2		3.586						
63-3		3.566						
63-4		3.546						
63-5		3.526						
63-6		3.506						
63-7		3.486						
63-8		3.466						
63-9		3.446						
63-10		3.426						
63-11		3.406						
63-12		3.386						
65-8		3.486	0	0	¼ mil Al	Al	1440 seconds	SO-212
66-8		3.486	0	0			1440 seconds	SO-212
67-2	1	3.486	0	-14.4			1440 seconds	SO-212
	2			- 7.2				
	3			0				
	4			+ 7.2				
	5			+14.4				
	6		+10.0	0				
68-6	1	3.486	+10.0	0			360 seconds	103-0
68-8	1	3.486	+10.0	0			720 seconds	103-0
68-10	1	3.486	+10.0	0			1440 seconds	103-0
69-12	1	3.486	0	+14.4			720 seconds	103-AO
	2			+ 7.2				
	3			0				
	4			- 7.2				
	5			-14.4				
70-12	1	3.486	0	+14.4			1080 seconds	103-AO
70-14	1	3.486	0	+14.4			1440 seconds	103-AO
70-16	1	3.486	0	+14.4			720 seconds	103-AO
	2			+ 7.2				
	3			0				
	4			- 7.2				
	5			-14.4				
71.6	1	3.486	0	0			720 seconds	SO-212
71-8	1	3.486	0	0			1080 seconds	SO-212

Table 12a - Photographic Exposure Conditions

Data Run Frame	Ex-pos. No.	Adjustable Housing Position (Inches	ϑ (Arc-Min)	ϕ (Arc-Min)	Filter Material	Source	Exposure Unit	Film Type
71-10	1	3.486	0	0	¼ mil Al	Al	1440 seconds	SO-212
71-12	1	3.486	0	0			1800 seconds	SO-212
71-14	1	3.486	0	-14.4			1080 seconds	SO-212
	2	↓	↓	- 7.2			↓	↓
	3			0				
	4			+ 7.2				
	5			+14.4				
72-1	1	3.486	0	-21.6			720 seconds	103-AO
	2	↓	↓	-14.4			↓	↓
	3			- 7.2				
	4			- 3.6				
	5			0				
	6			+ 3.6				
	7			+ 7.2				
	8			+14.4				
	9			+21.6				
72-2	1	3.486	-10.0	-21.6			720 seconds	103-AO
	2	↓	↓	-14.4			↓	↓
	3			- 7.2				
	4			- 3.6				
	5			0				
	6			+ 3.6				
	7			+ 7.2				
	8			+14.4				
	9			+21.6				
72-3	1	3.486	-10.0	+21.6			720 seconds	103-AO
72-4	1	3.486	+10.0	+21.6			720 seconds	103-AO
	2	↓	↓	+14.4			↓	↓
	3			+ 7.2				
	4			+ 3.6				
	5			0				
	6			- 3.6				
	7			- 7.2				
	8	↓	↓	-14.4	↓	↓	↓	↓
	9			-21.6				

Table 12b - Photographic Exposure Conditions

Data Run Frame	Expos. No.	Adjustable Housing Position (Inches)	ϑ (Arc-Min)	ϕ (Arc-Min)	Filter Material	Source	Exposure Unit	Film Type
72-5	1	3.476	0	-21.6	¼ mil Al	Al	720 seconds	103-AO
	2			-14.4				
	3			- 7.2				
	4			- 3.6				
	5			0				
	6			+ 3.6				
	7			+ 7.2				
	8			+14.4				
	9			+21.6				
72-6	1	3.466		+21.6				
	2			+14.4				
	3			+ 7.2				
	4			+ 3.6				
	5			0				
	6			- 3.6				
	7			- 7.2				
	8			-14.4				
	9			-21.6				
72-7	1	3.446		-21.6				
	2			-14.4				
	3			- 7.2				
	4			- 3.6				
	5			0				
	6			+ 3.6				
	7			+ 7.2				
	8			+14.4				
	9			+21.6				
72-8	1	3.486		0			720 seconds	103-AO
72-9	1	3.486		0			360 seconds	103-AO
72-10	1	3.486		0			180 seconds	103-AO

Table 12c - Photographic Exposure Conditions

Data Run Frame	Ex-pos. No.	Adjustable Housing Position (Inches)	(Arc-Min)	(Arc-Min)	Filter Material	Source	Exposure Unit	Film Type
73-8	1	3.486	0	0	¼ mil Al	Al	1800 seconds	SO-212
73-10	1	3.486	0	+20.0			600 seconds	SO-212
	2			+10.0				
	3			0				
	4			-10.0				
	5			-20.0				
	6		+10.0	-20.0				
	7		-10.0	-20.0				
	8		+10.0	+20.0				
	9		-10.0	+20.0				

Table 12d - Photographic Exposure Conditions

minutes and 20 arc minutes off the telescope axis in the azimuth (ϕ) direction, and could be moved forward from the focal plane by a chain drive screw adjustment to 0.020" and 0.040". The image was examined by sweeping the telescope in 0.25 arc minute steps via step motors.

A point source was made up of an aluminum anode operated at 6.0 KV and 50 ma with a 0.25" diameter pinhole in front of the source. The telescope mode was no filter (blank on position #4 of filter wheel) and open shutter. Gas flow proportional counters were used to measure the incident X-ray intensity and focused X-rays through the 0.010" pinhole. Both counters were operated at 1400 V with a gain of 280 and a P-10 gas flow rate of 0.075 SCFH. Both used 0.25-mil-thick Mylar windows.

Data was acquired by sweeping the telescope through the azimuth ($\Delta\phi$) and elevation ($\Delta\theta$) directions with the pinhole situated in the center of the focal plane (at d=0, ϕ=0, θ=0). The telescope was then swept in an azimuth direction in one arc minute steps (via the telescope platform step motors) while the "elevation" and "d" value remained fixed. At each one arc minute interval the values of the incident radiation and reflected radiation were recorded and plotted, as indicated in Figure 26. This process was then repeated keeping the "azimuth" and "d" value fixed and sweeping the elevation in one arc minute intervals. When the position of the peak value of the reflected

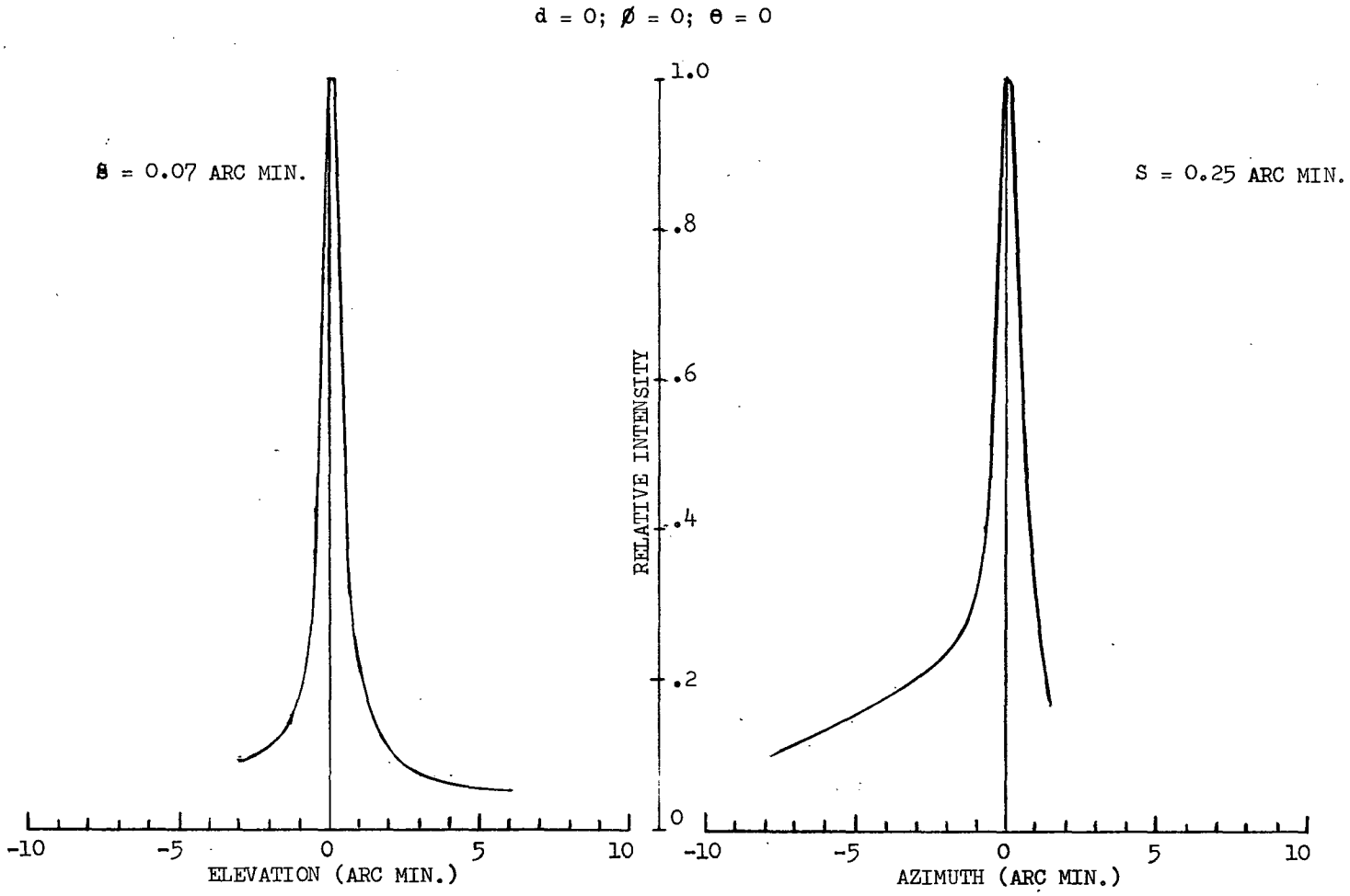

Figure 26 - SO-56-4 Telescope Point Source Test--Pinhole at Focal Point

radiation was found, the sweeping procedure in azimuth and elevation was repeated, this time in 0.25 arc minute intervals, to provide a more absolute determination of the peak value. The focal plane fixture was then "defocused"by changing the "d" values to -0.020" and -0.040" and also placing ϕ to the 10' and 20' positions. In each case the sweeping process in elevation and azimuth was made providing ten curves as given by Figures 26 through 30.

Table 13 summarizes the results obtained in these tests. The efficiency is computed by measuring the flux incident on the telescope and comparing that with the intensity recorded behind the pinhole. The efficiency represents the intensity from a 20 arc second source that is focused on a spot of 28 arc seconds diameter. Both absorption in the mirror and scattering of intensity away from the main beam will adversely affect the efficiency measured. The value, S, is defined here as the difference between the observed peak width and the calculated width (0.8 arc minute.) The widths in the elevation were different from those in azimuth indicating non-symmetry in the images.

Changes in the distance, d, seemed to have little effect on either the efficiency or the width of the curves. This is probably due to the poor overall performance of the telescope. In going off-axis, however, the efficiency dropped rapidly by about half at 20 arc minutes off axis, and the image began to

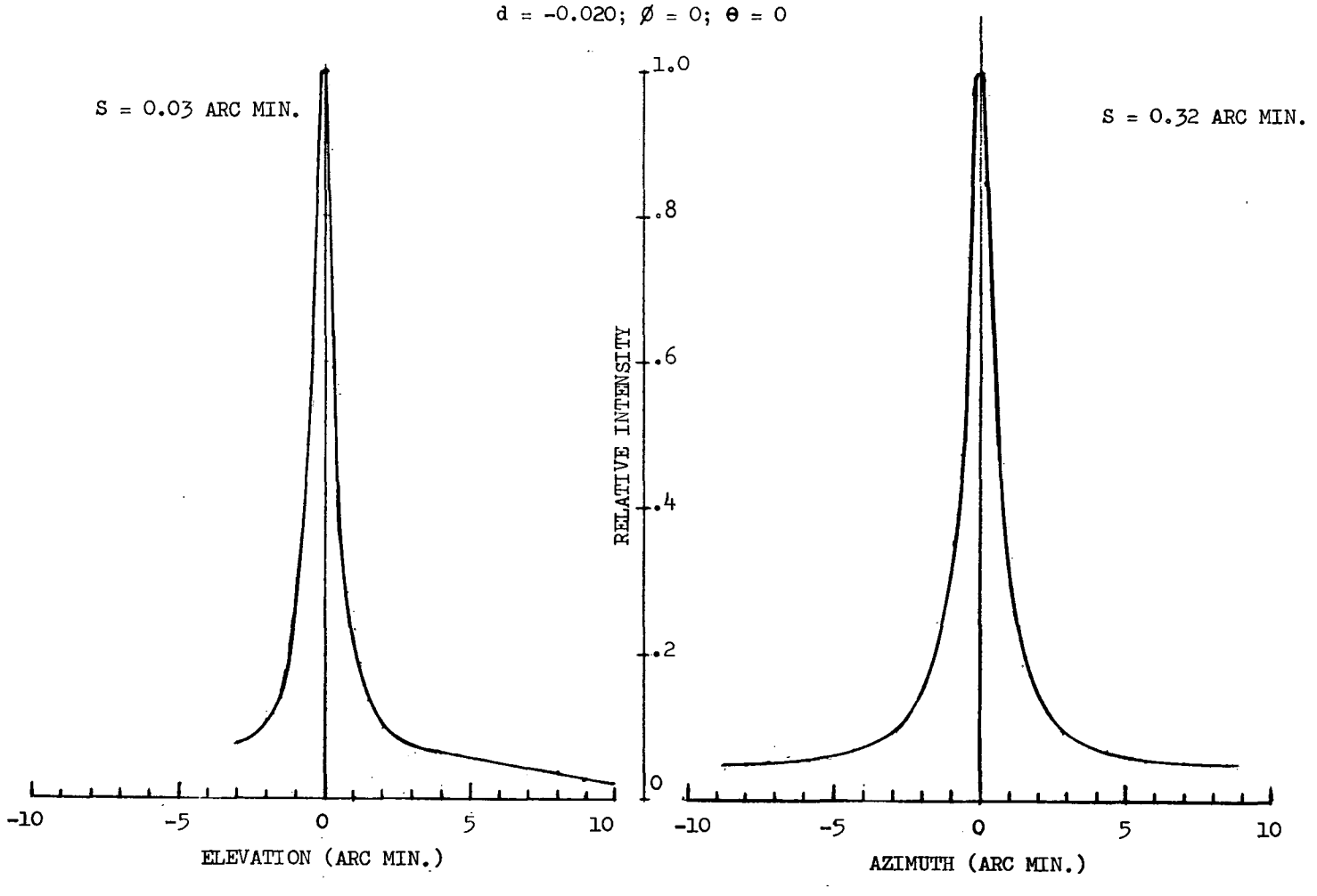

Figure 27 - SO-56-4 Telescope Point Surce Test-Pinhole Offset 0.020 Inches Inward

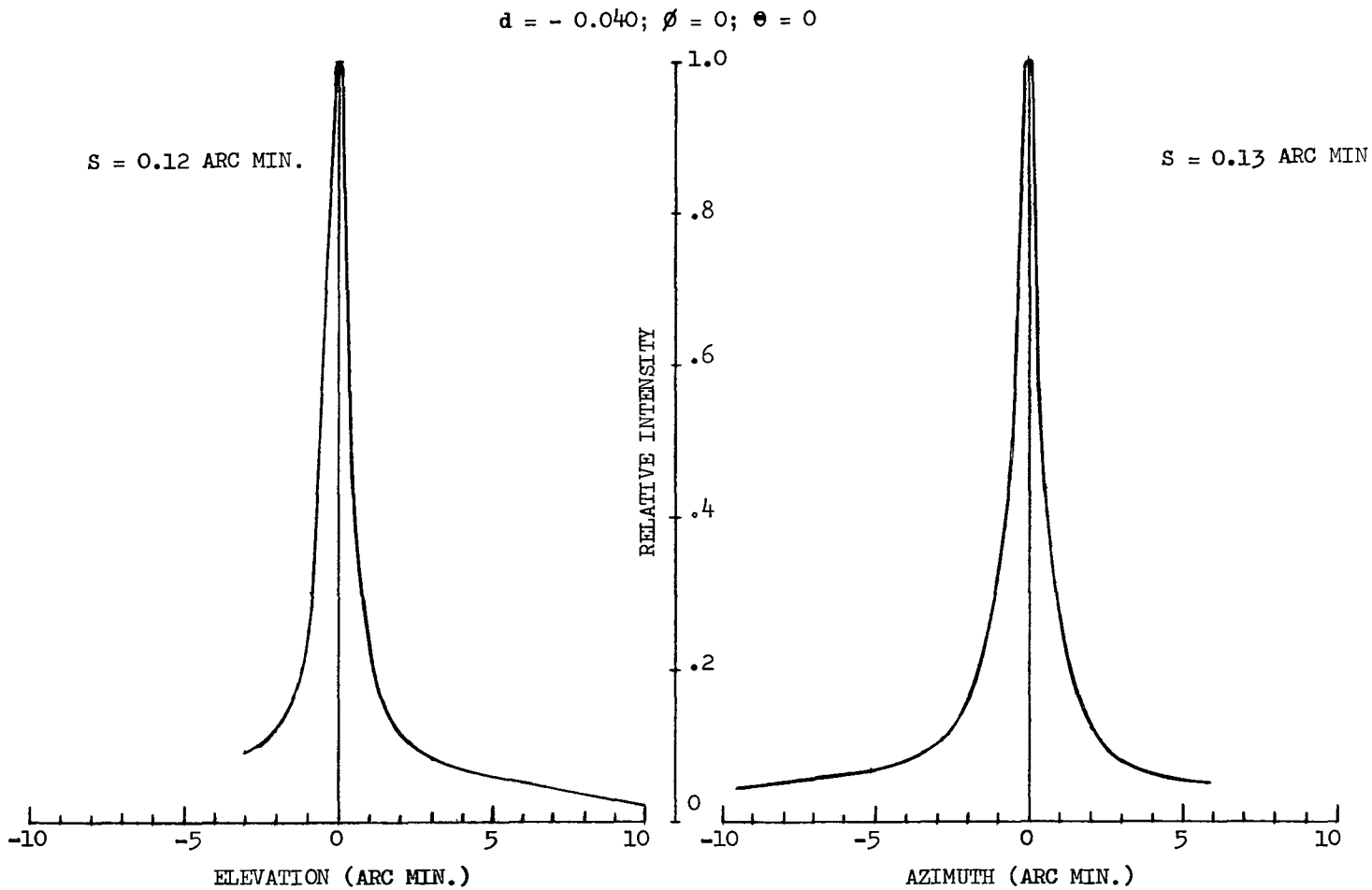

Figure 28 - SO-56-4 Telescope Point Source Test-Pinhole Offset 0.040 Inches Inward

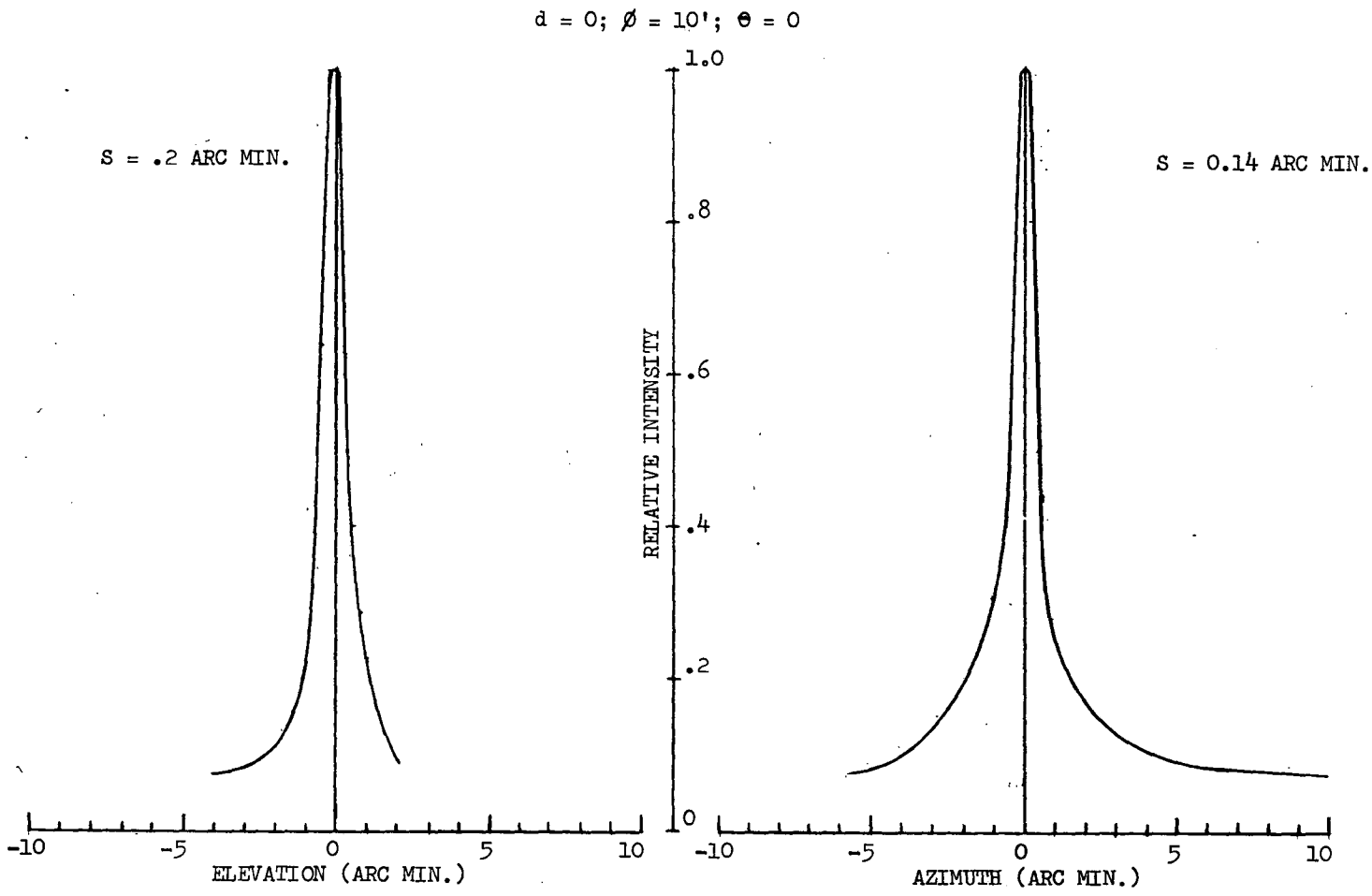

Figure 29 - SO-56-4 Telescope Point Source Test-Pinhole Offset 10 Arc Min. from Axis

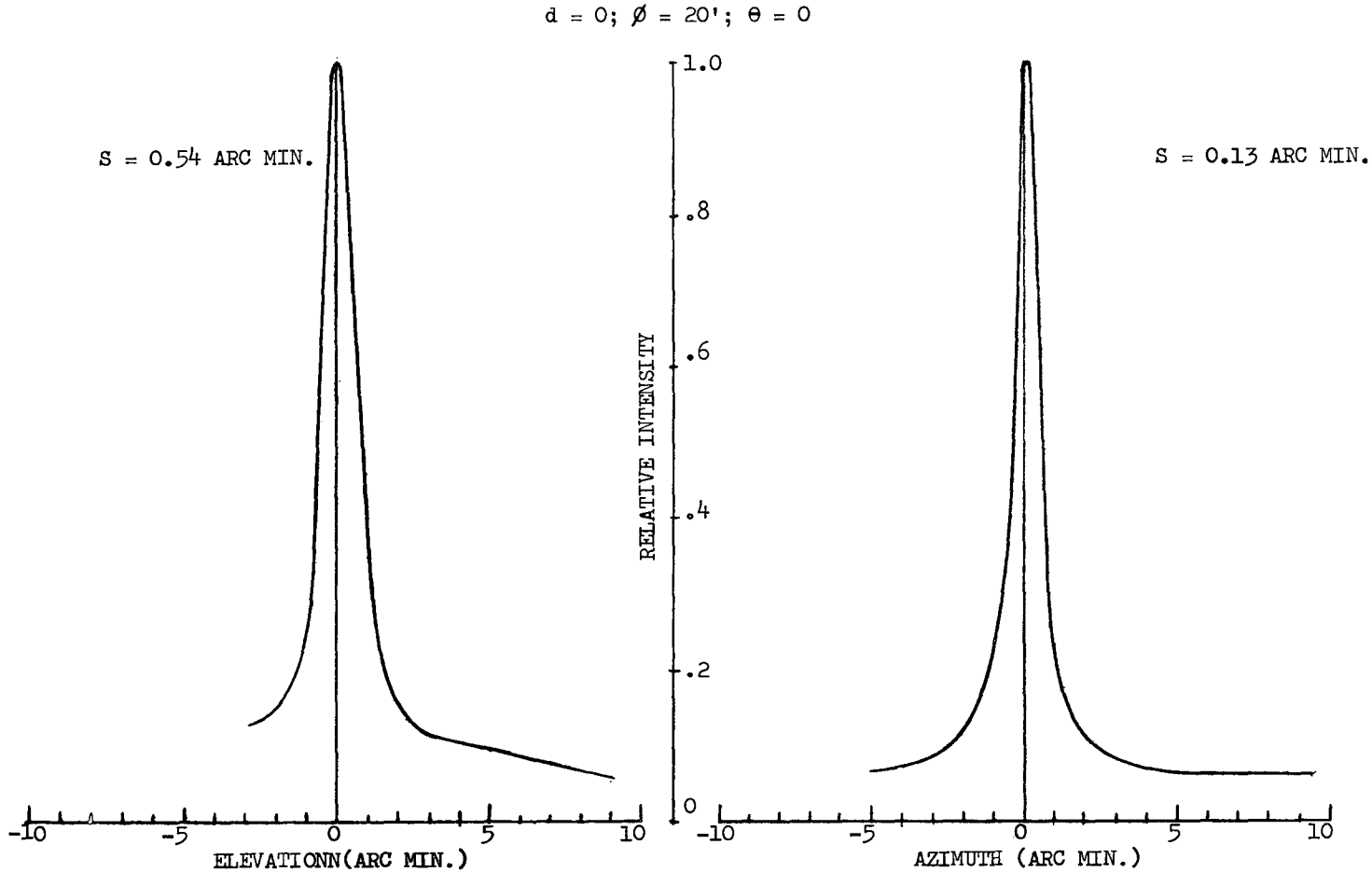

Figure 30 - SO-56-4 Telescope Point Source Test-Pinhole Offset 20 Arc Min. from Axis

elongate in the azimuth (radial) direction. These effects were also noted in the photographs. The effect of the wings must dominate the photographs since better resolutions were attained in the pinhole images than in resolution chart photographs.

Table 13

Figure	26		27		28		29		30	
d, ϕ, θ	0, 0, 0		-0.02", 0, 0		-0.04", 0, 0		0, 10', 0		0, 20', 0	
Direction	$\Delta\theta$	$\Delta\phi$	$\Delta\theta$	$\Delta\phi$	$\Delta\theta$	$\Delta\phi$	$\Delta\theta$	$\Delta\phi$	$\Delta\theta$	$\Delta\phi$
Efficiency in Percent	0.063	0.060	0.063	0.061	0.060	0.064	0.045	0.049	0.029	0.037
S in Arc Min	0.25	0.07	0.32	0.03	0.13	0.12	0.14	0.20	0.13	0.54

NEW TECHNOLOGY

In this section, a description will be given of the apparatus used for the X-ray scattering measurements. The vacuum system consisted of three stainless steel chambers,each 24 inches in diameter and 12 inches high. The three chambers were interconnected by 6 inch I.D. stainless steel tubing. The distance between the center line of each chamber was 17.2 feet. The middle chamber housed the sample and secondary detector with one end chamber enclosing the X-ray source and the other end chamber enclosing the detector used for measuring the reflected X-ray beam. Each of the end chambers have their own pumping system consisting of a mechanical pump used for either roughing down the chambers and line or as a forepump for the 6 inch diffusion pump. Above each diffusion pump is a cold trap which is filled with liquid nitrogen to minimize any oil from backstreaming into the main vacuum system. The experimental configuration of the X-ray scattering measurement equipment is shown in Figure 31.

Two X-ray sources were used in this test which were aluminum (8.34 $\mathring{A}$) and carbon (44 $\mathring{A}$). Although there was some tungsten deposited on the sources, single channel analyzers were used to eliminate counting the higher energy X-rays produced by the tungsten. For aluminum, the anode voltage was 3.5 KV and the anode current was 20 - 30 ma; whereas for the carbon runs, the

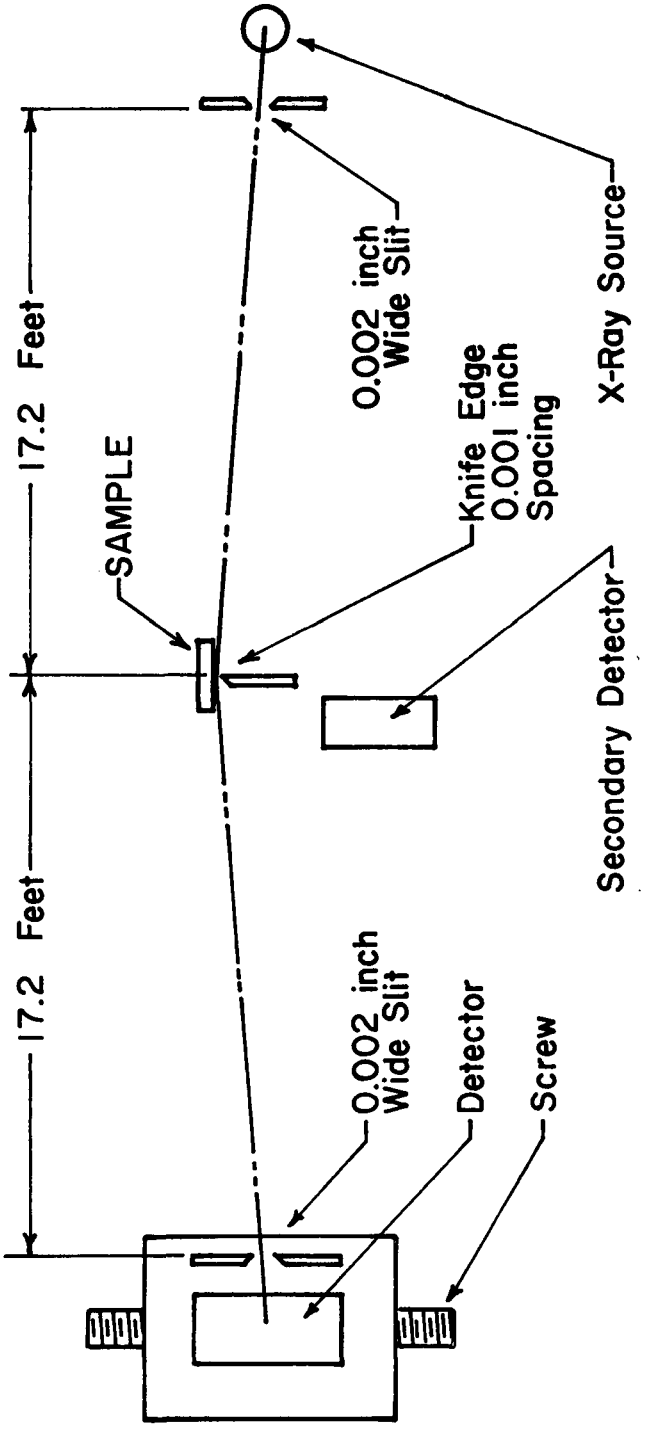

Figure 31 - X-ray Scattering Measurement Equipment

anode voltage was 1.4 KV and the anode current was 30 ma. The filament was essentially a line source which was .005 inch diameter tungsten wire. Directly in front of the source was a .002 inch wide slit. The purpose of this slit and the slits at the sample and detector were to yield a theoretical FWHM value of the scattering curves which, when compared to the experimental FWHM value, would give a value of the amount of scattering produced by the surface imperfections of the sample.

In the middle chamber, 17.2 feet away from the source, the sample was mounted in the sample holder. The sample holder had a replaceable front mount which could hold either 2 inch or 1.5 inch diameter samples. The sample holder could be rotated in either direction in one arc minute steps. The knife edge spacing was achieved by placing shims between the sample and the knife edge and then spring loading the sample in this position. From geometrical considerations, the knife edge spacing at the sample must be doubled to give the true theoretical value for this spacing. A secondary detector or monitor detector was placed adjacent to the sample holder. The purpose of this detector was to monitor the direct beam from the X-ray source so that any variations that occurred at the source could be taken into account in the final analysis of the scattering data. A beam stop with a one inch diameter hole was placed directly in front of the sample between the sample and the detector end

of the system. The beam stop helped reduce the amount of X-rays scattered from the chamber walls or X-rays from the direct beam from reaching the primary detector.

In the end chamber, 17.2 feet from the sample the primary detector was placed on a mount that could be moved along a screw. By proper choice of step motor, gears, and screw thread size, the detector could be translated across the scattered X-ray beam in 0.1 arc second intervals. The detector was a flow type proportional counter with a replaceable window. When making the 8.34 Å aluminum runs, the window in the detector was ¼ mil aluminum. During the 44 Å carbon runs, the ¼ mil aluminum window was replaced with a 2 micron thick Makrofol window supported by nickel mesh. A .002 inch or .004 inch wide slit was placed directly in front of the window of the detector.

Initially, the system was aligned by means of a laser so that the angle of incidence between the sample and the X-ray source was the proper value, in this case either 0.5^{o}, 0.92^{o}, 2^{o} or 4^{o}. After the sample and the primary detector were put in position, the chamber was closed and the pressure reduced to approximately 8×10^{-6} Torr. The high voltage for the X-ray source was then turned on and the scattered X-ray beam was located. After the peak of the scattered beam was located, the primary detector was positioned +30 arc seconds from the peak. A typical run consisted in translating the detector and slit

across the scattered X-ray beam in 1 arc second intervals and counting for 100 seconds at each point from +30 arc seconds to -30 arc seconds.

CONCLUSIONS

The optical flat data can only be interpreted with a thorough knowledge of the origin of the samples. We do not have this information. On the other hand, there are some general trends shown by the data. They are:

1. The magnitude of scattering of X-rays was greater at 44 Å than it was at 8 Å.
2. The scattering was large in magnitude at small angles and decreased as the glancing angle of incidence increased until the critical reflecting angle was passed. The scattering increased again past this point. This was borne out by the values at 8 Å where the optimum glancing angle of incidence was 0.92°. Both 2° and 4° were more suitable glancing angles of incidence at 44 Å.
3. The samples that show small amounts of scattering at 44 Å did not necessarily work well at 8 Å and conversely. The sample having the least scattering at 8 Å was number 6, and number 5 was a close second. At 44 Å, nine samples had small scattering values.
4. Performance of metal optical surfaces was comparable with that of glass surfaces. At 8 Å, the glass surfaces were superior, but at 44 Å several metal surfaces showed about the same scattering as glass.

The tests of the Kanigen coated telescope mirror were done in the same way as previous tests[1-3] so that comparisons with the quartz telescope mirrors can be made. They are:

1. This telescope showed excessive scattering of X-rays and the performance in all tests was substantially poorer than that of the quartz mirrors. The angular resolution in the photographs, the long exposure times required, and the very low efficiency values all consistently supported this conclusion.
2. The best photographic angular resolution attainable with this telescope was of the order of 15 arc seconds.
3. The images showed some asymmetry with the azimuth component of the image elongated relative to the elevation component. This asymmetry increased off-axis.
4. The excessive scattering resulted in an overall reflecting efficiency of .06% at 8 $\mathring{A}$. This is three orders of magnitude less than expected.

RECOMMENDATIONS

The following areas should be investigated in order to better understand how to predict performance of future mirrors:

1. Additional optical flat samples should be tested in the same way to investigate polishing techniques.
2. Orientation effects should be investigated by measurement of the scattering of a sample(s) as it is turned in the holder. The positions tested should be 0, 30, 60, 90, 120, and 150 degrees.
3. Repeatability of the curves should be investigated by periodically measuring a sample under as nearly identical conditions as possible. The entire set-up procedure should be required for this test. Effects of sustained vacuum exposure of the samples should also be investigated.
4. Models of surfaces should be investigated theoretically and equations for these models should be derived. Predicted scattering values should be compared with calculated values.
5. The angles of incidence at 8 $\mathring{A}$ should be smaller in magnitude (e.g., 0.5°, 0.92°, 1.5°, 2.0°).
6. The number of wavelengths should be expanded substantially in at least one case (e.g., 8.34, 9.9, 13.3, 17.6, 27.3, 44, and 67 $\mathring{A}$).

7. The angular dependence of scattering should be investigated through the critical angle in small angular intervals (e.g., 1 or 2 arc minutes). This can be done very accurately if the vacuum is not broken. The system has a range of approximately 1^{o} for this test.
8. Reflecting efficiency should be investigated for all samples.
9. The Kanigen coated beryllium mirror should be repolished and tested afterwards.

REFERENCES

1. R. S. Wriston, Technical Report No. ED-2002-907-1, NASA Contract NAS8-24000, September 1969, "S-056 Quartz Mirror Test, Flight Optics B".

2. R. S. Wriston, Technical Report No. ED-2002-907-2, NASA Contract NAS8-24000, October 1969, "S-056 Quartz Mirror Test, MSFC Mirror".

3. R. S. WRiston, Technical Report No. ED-2002-907-3, NASA Contract NAS8-24000, February 1970, "W-056 Quartz Mirror Test, Flight Optics A".

4. Private Discussions with P. W. Sanford of UCL after Tests of their OAO-C X-ray Telescopes at the Martin Marietta Test Facility.

5. W. Ehrenberg, J. Opt. Soc. Am. 39, 746 (1949).

6. S. B. Elliott, X-ray Optics and X-ray Microanalysis, H. H. Pattee, V. E. Cosslett, and A. Engstrom, Ed. (Academic Press, N. Y., 1963), p. 215.

7. J. B. Schroeder and R. B. Klimasewski, Appl. Opt. 7, 1921 (1968).